Title

Dual-Sized Microparticle System for Generating Suppressive Dendritic Cells Prevents and Reverses Type 1 Diabetes in the Nonobese Diabetic Mouse Model

Journal

ACS Biomaterials Science & Engineering, 5(5)

ISSN

2373-9878

Authors

Lewis, Jamal S
Stewart, Joshua M
Marshall, Gregory P
et al.

Publication Date

2019-05-13

DOI

10.1021/acsbiomaterials.9b00332

Peer reviewed

ACS Biomaterials SCIENCE & ENGINEERING

Article

Cite This: ACS Biomater. Sci. Eng. 2019, 5, 2631−2646

pubs.acs.org/journal/abseba

Dual-Sized Microparticle System for Generating Suppressive Dendritic Cells Prevents and Reverses Type 1 Diabetes in the Nonobese Diabetic Mouse Model

Jamal S. Lewis,[†,∥,⊥,#] Joshua M. Stewart,[†,#] Gregory P. Marshall,[∥] Matthew R. Carstens,[†] Ying Zhang,[†] Natalia V. Dolgova,[†] Changqing Xia,[‡] Todd M. Brusko,[‡] Clive H. Wasserfall,[‡] Michael J. Clare-Salzler,[‡] Mark A. Atkinson,[‡,§] and Benjamin G. Keselowsky*[,†,‡]

[†]J. Crayton Pruitt Family Department of Biomedical Engineering, University of Florida, 1275 Center Drive, Gainesville, Florida 32611, United States

[‡]Department of Pathology, Immunology and Laboratory Medicine, University of Florida, 1600 SW Archer Road, Gainesville, Florida 32611, United States

[§]Department of Pediatrics, University of Florida, 1600 SW Archer Road, Gainesville, Florida 32611, United States

[∥]OneVax, LLC, 12085 Research Drive, Alachua, Florida 32615, United States

[⊥]Department of Biomedical Engineering, University of California—Davis, One Shields Avenue, Davis, California 95616, United States

Supporting Information

ABSTRACT: Antigen specificity is a primary goal in developing curative therapies for autoimmune disease. Dendritic cells (DCs), as the most effective antigen presenting cells in the body, represent a key target to mediate restoration of antigen-specific immune regulation. Here, we describe an injectable, dual-sized microparticle (MP) approach that employs phagocytosable ∼1 μm and nonphagocytosable ∼30 μm MPs to deliver tolerance-promoting factors both intracellularly and extracellularly, as well as the type 1 diabetes autoantigen, insulin, to DCs for reprogramming of immune responses and remediation of autoimmunity. This poly(lactic-*co*-glycolic acid) (PLGA) MP system prevented diabetes onset in 60% of nonobese diabetic (NOD) mice when administered subcutaneously in 8 week old mice. Prevention of disease was dependent upon antigen inclusion and required encapsulation of factors in MPs. Moreover, administration of this "suppressive-vaccine" boosted pancreatic lymph node and splenic regulatory T cells (Tregs), upregulated PD-1 on $CD4^+$ and $CD8^+$ T cells, and reversed hyperglycemia for up to 100 days in recent-onset NOD mice. Our results demonstrate that a MP-based platform can reeducate the immune system in an antigen-specific manner, augment immunomodulation compared to soluble administration of drugs, and provide a promising alternative to systemic immunosuppression for autoimmunity.

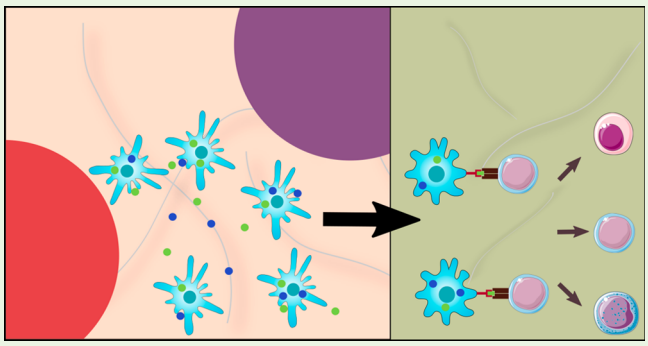

KEYWORDS: *type 1 diabetes, treatment, PLGA, microparticle, biomaterial, dendritic cell, trafficking*

1. INTRODUCTION

Type 1 diabetes (T1D) is an autoimmune disease classically characterized by T cell mediated destruction of insulin-producing β-cells in the pancreas.[1] Disease incidence is increasing annually, with current estimates suggesting roughly 1.5 million people in the United States and 490 000 children below the age of 15 worldwide suffering from T1D.[2] Despite best practice management with insulin therapy, patients experience a 10-fold increased risk for cardiovascular disease and up to 30% suffer from life-threatening, chronic kidney disease among other comorbid complications.[3−5] To date, there is no cure for T1D. However, a myriad of interventions have been explored in clinical trials with varied success. Therapies including islet transplantation, monoclonal antibody immunotherapy (e.g., anti-CD3, anti-CD20), anti-thymocyte globulin based therapies, and autologous stem cell transfusion have shown promise in recent years.[6−11] While initial reports have been optimistic, significant proportions of individuals in each of the clinical trials revert to insulin dependency a few months or years removed from therapy.[12−14] Furthermore, the use of systemic immunosuppression (e.g., cyclosporin) occasionally applied in novel T1D clinical trials diminishes long-

Received: March 7, 2019
Accepted: March 26, 2019
Published: March 26, 2019

DOI: 10.1021/acsbiomaterials.9b00332
ACS Biomater. Sci. Eng. 2019, 5, 2631−2646

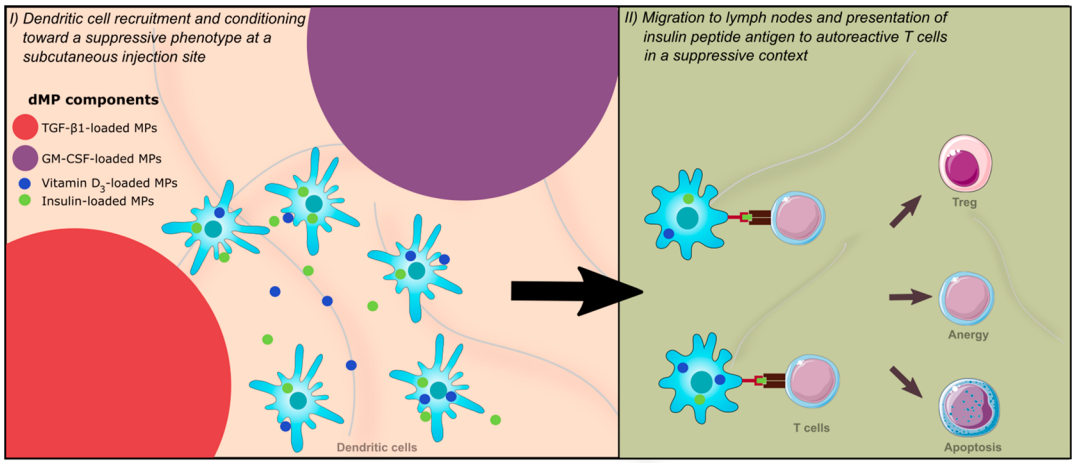

Figure 1. Schematic of the dual-sized microparticle (dMP) system. The dMP formulation is an injectable platform that provides sustained extracellular release of a DC chemokine, GM-CSF, and a protolerogenic factor, TGF-β1, via ~30 μm nonphagocytosable MPs to recruit and condition DCs at a subcutaneous injection site. Concurrently, ~1 μm phagocytosable MPs encapsulating antigen, denatured insulin, and a tolerizing agent, vitamin D_3, provide targeted intracellular delivery to the locally recruited DCs in order to promote presentation of the T1D autoantigen in a tolerogenic context.

term prospects, as patients have increased risk for opportunistic infections and cancer development.[15] These limitations have renewed interest in developing antigen-specific therapies to treat T1D.

In order to modulate the adaptive, antigen-specific arm of immunity, a number of immunotherapies have been developed to target antigen presenting cells (APCs).[16,17] Dendritic cells (DCs) are the most effective subset of APCs in directing the adaptive immune response.[18] In response to inflammatory signals such as pathogen associated molecular patterns or damage associated molecular patterns, DCs undergo phenotypic and functional changes that serve to promote T cell activation, including upregulation of chemokine receptors to encourage migration to lymph nodes (LN; e.g., CCR7), secretion of inflammatory cytokines (e.g., IL-12), and upregulation of surface co-stimulatory markers (e.g., CD80, CD86).[18] In the context of T1D, accumulating evidence has suggested that aberrant DC activation plays a pivotal role in T1D pathogenesis.[19,20] However, DCs can also act as agents of tolerance, suppressing the pathways that potentiate autoimmunity. Tolerogenic DCs can establish and maintain peripheral tolerance by a number of mechanisms including induction of T cell anergy, promotion of Treg differentiation, and effector T cell depletion.[21] Therapies utilizing tolerogenic DCs are now under investigation for use as live "negative vaccines" for antigen-specific autoimmune immunotherapy.[22] Although early results in animal studies and clinical trials are promising, widespread translation of this cell-based vaccination approach could prove onerous due to a number of limitations. Notably, ex vivo procedures required to generate tolerogenic DCs lead to high manufacturing costs, significant regulatory complications, and inefficient DC migration to LNs following transfusion (<3% of DCs).[23,24]

These drawbacks have inspired development of biomaterial-based strategies for in vivo conditioning of DCs.[17,25−27] For instance, Phillips et al. demonstrated that subcutaneously injected poly(lactic-*co*-glycolic acid) (PLGA) microparticles (MPs) loaded with antisense oligonucleotides against co-stimulatory molecules CD40/80/86 were taken up by DCs and protected nonobese diabetic (NOD) mice from T1D.[28] Similarly, Maldonado et al. showed that administration of PLGA nanoparticles encapsulating antigen and rapamycin, a potent immunosuppressant, localized with DCs and macrophages in draining LNs (dLNs) and improved therapeutic outcomes in a host of immune-mediated conditions including allergic hypersensitivity, antibody responses against factor VIII in hemophilia A mice, and a mouse model for multiple sclerosis (MS).[29] Interestingly, it was recently demonstrated that PLGA MPs alone can have latent, immunosuppressive capabilities and may be able to contribute to the dampened immune responses.[30]

Previously, our group demonstrated that subcutaneous injection of a dual-sized, biodegradable PLGA MP system, comprising two ~1 μm phagocytosable MPs (vitamin D_3 (VD_3) and insulin B_{9-23} peptide-loaded MPs) and two ~30 μm nonphagocytosable MPs (transforming growth factor β1 (TGF-β1)-loaded MPs and granulocyte-macrophage colony-stimulating factor (GM-CSF)-loaded MPs), protected 4-week-old NOD mice from T1D.[31] Additionally, we have demonstrated that this dual-sized MP (dMP) system can be used in a plug-and-play manner in other autoimmune models, as substitution for the disease-relevant antigen also mitigated disease in a mouse model of MS.[32] The main objective behind the dMP system (Figure 1) is that the large, nonphagocytosable MPs in subcutaneous tissue provide extracellular release of a DC chemokine (GM-CSF) and protolerogenic cytokine (TGF-β1) that recruit and tolerize DCs, respectively.[33,34] Concurrently, phagocytosable MPs at the subcutaneous injection site containing insulin (denatured, nonmetabolically active), a primary autoantigen for T1D,[35] and an additional immunomodulatory factor, vitamin D_3(VD_3), are phagocytosed by locally recruited DCs for antigen processing and presentation and VD_3 delivery to its nuclear receptor, respectively.[36] Hence, this dMP system was designed to promote presentation of autoantigen in a tolerogenic context to reeducate aberrant autoreactivity. The observed efficacy of the dMP platform administered to 4-week-old NOD mice, though significant from control groups, was suboptimal as only 40% of mice remained diabetes free after 32 weeks of age.[31] Additionally, treatment in 4-week-old NOD mice, which are prediabetic and do not typically display significant inflammatory leukocyte infiltration in pancreatic islets (insulitis), does

DOI: 10.1021/acsbiomaterials.9b00332
ACS Biomater. Sci. Eng. 2019, 5, 2631−2646

not accurately represent pathology of human T1D at the time of diagnosis. Thus, treatment in NOD mice that have more advanced insulitis or are overtly hyperglycemic represents models that are more clinically relevant. Herein, we describe our efforts to re-engineer and improve the dMP system in late-stage diabetes prevention and investigate the capacity of our platform to reverse T1D in NOD mice.

2. MATERIALS AND METHODS

2.1. Microparticle Fabrication and Characterization. Poly(lactic-*co*-glycolic acid) (MW ∼ 44 000 g/mol; Corbion Purac, Gorinchem, The Netherlands) MPs were fabricated by standard oil-in-water single emulsion or water-in-oil-in-water double emulsion methods. All factors were separately encapsulated in distinct MPs to facilitate ease of omission/inclusion of individual drugs. Briefly, phagocytosable MPs were loaded with 1-α,25-dihydroxyvitamin D_3 (VD_3; Thermo Fisher Scientific, Waltham, MA) or denatured human recombinant insulin (Sigma-Aldrich, St. Louis, MO) while non-phagocytosable MPs encapsulated TGF-β1 or GM-CSF (Millipore Sigma).

Insulin was rendered inactive by chemical means and heat denaturation. First, insulin was reconstituted in ultrapure water (Barnstead GenPure, Thermo Fisher Scientific) and 1 M HCl added dropwise to promote solubility of insulin in solution (pH ∼ 2.5). Peptide disulfide bonds were cleaved by adding 10 mM 2-mercaptoethanol (Sigma-Aldrich). This solution was subsequently incubated in a water bath at 95 °C for 5 min to ensure complete denaturation of insulin. After cooling to room temperature, 0.1 M NaOH was added dropwise until pH reached between 7.0 and 7.5 without inducing protein aggregation out of solution. Lastly, this solution was filtered through a low-binding 0.22 μm filter and concentration confirmed by spectrophotometry (NanoDrop ND-1000, Thermo Fisher Scientific) against a standard curve.

Phagocytosable MPs were fabricated by dissolving 500 mg of PLGA in methylene chloride at a 5% w/v ratio. 50 μg of VD_3 in 1 mL of methanol (Thermo Fisher Scientific) was loaded directly into the methylene chloride/PLGA solution and set to shake at 150 rpm for 10 min. This solution was then added to 50 mL of 5% w/v poly-vinyl alcohol (PVA; MW ∼ 15 000 g/mol; Themo Fisher Scientific) and homogenized at 35 000 rpm for 180 s using a tissue-miser homogenizer (Thermo Fisher Scientific) to form an oil-in-water emulsion. The microparticle solution was subsequently added to a beaker of 100 mL of 1% PVA and set to stir for 4−6 h for solvent evaporation and microparticle hardening to occur. For water-soluble denatured insulin MPs, 13 mg of protein in 2 mL of PBS was added to the 5% methylene chloride/PLGA solution and homogenized at 35 000 rpm for 120 s to form a primary emulsion. This emulsion was added to 50 mL of 5% PVA and homogenized again at 35 000 rpm for 180 s to form the secondary emulsion and added to 100 mL of stirring 1% PVA.

Nonphagocytosable MPs encapsulating TGF-β1 and GM-CSF were fabricated by first dissolving 500 mg of PLGA in methylene chloride at a 20% w/v ratio. Human TGF-β1 was reconstituted in 10 mM hydrochloric acid and 2 mg/mL bovine serum albumin in 250 μL of PBS, and recombinant mouse GM-CSF was reconstituted in 400 μL of PBS. Protein solutions were added to the methylene chloride/PLGA solution and vortexed at the highest setting (∼3200 rpm) for 30 s to generate the primary emulsion. This emulsion was added to 5 mL of 2.5% PVA and vortexed again at 3200 rpm for 60 s to form the secondary emulsion and finally added to 100 mL of stirring 1% PVA. Either methanol or PBS was used to generate unloaded MPs, depending on the control group being fabricated.

After 4−6 h, solutions were centrifuged at 10 000*g* for 10 min to collect MPs and washed three times with ultrapure water. The resultant MPs were then flash-frozen in liquid nitrogen and lyophilized for 24 h. The MPs were stored at −20 °C until their use.

Size distributions of nonphagocytosable MPs were measured by the Beckman Coulter LS13320 (Beckman Coulter Inc., Brea, CA) and phagocytosable MPs by the Microtrac Nanotrac dynamic light scattering particle analyzer (Microtrac, Montgomery, PA). Particle morphology was characterized by scanning electron microscope (FEG-SEM JEOL JSM-6335F).

Loading efficiency of MPs was measured by dissolving MPs in methylene chloride (Thermo Fisher Scientific, NJ, USA) and extracting proteins (insulin, TGF-β1, GM-CSF) with water or hydrophobic drugs (VD_3) with methanol (Thermo Fisher Scientific). Following evaporation, residual drug remaining in the tube was concentrated in a known, small quantity of dimethyl sulfoxide or water and measured by spectrophotometer or ELISA.

Release kinetics were determined by aliquoting 25 mg of MPs into microtubes containing 200 μL of simulated body fluid (SBF; formulation described by Oyane et al.[37] which has ion concentrations almost equal to those of human plasma and is therefore a representative dissolution medium to assess MP release kinetics in vitro). All MP samples were sealed and transferred to a rotary shaker maintained at 37 °C. At 1, 3, 5, 7, 14, and 28 days, samples were pelleted by centrifugation at 10 000*g* for 10 min and supernatants collected and stored at −20 °C. The remaining MP pellets were then resuspended in 200 μL of fresh SBF. At the final time-point, supernatants were analyzed by either spectrophotometry (NanoDrop; for VD_3 MP and insulin MP) or ELISA (BD Biosciences, San Jose, CA; for TGF-β1 MP and GM-CSF MP).

2.2. Experimental Animals. Female NOD/ShiLtj, C57BL/6, and Balb/c mice, ages 6−8 weeks, were purchased from either Jackson Laboratory (Bar Harbor, ME) or University of Florida Animal Care Services (ACS) (Gainesville, FL). All animals were housed in specific pathogen free-environment in University of Florida ACS facilities and used in accordance with detailed experimental protocols approved by University of Florida Institutional Animal Care and Use Committee (IACUC).

2.3. In Vitro Microparticle-Induced DC Suppressive Phenotype. Dendritic cells were obtained from 8- to 12-week-old, female, C57BL/6 mice using a modified 10 day protocol, as previously described.[38,39] DCs were incubated with MPs at 37 °C for 48 h prior to flow cytometric analysis. Phagocytosable MPs (VD_3 MP) were added at a 10:1 MP:DC ratio. Concomitantly, an amount of 10 mg of nonphagocytosable MPs (TGF-β1 MP) was incubated at a mass determined by loading and release kinetics to generate a TGF-β1 concentration (∼50 ng/mL TGF-β1) high enough to generate Tregs.[40] GM-CSF MPs were not included, as DC conditioning media already contained GM-CSF at concentrations similar to that released by fabricated MPs. Untreated immature DCs (iDC), 1 μg/mL lipopolysaccharide (LPS; Sigma) stimulation, and unloaded MPs were included as controls. After 48 h of incubation with MPs, DCs were washed with phosphate buffered saline (PBS; Thermo Fisher Scientific) three times to remove free MPs and lifted with 5 mM Na_2EDTA at 37 °C for 20 min. Subsequently, cells were stained, and DC phenotype was characterized by flow cytometry. Dendritic cell maturation resistance was assessed by stimulating DCs with 1 μg/mL LPS for 24 h following the MP incubation and washing steps.

2.4. Mixed Lymphocyte Reaction with MP-Treated DCs. $CD4^+$ T cells were purified from the spleens of 8-week-old Balb/c mice by negative selection using Miltenyi $CD4^+$ T cell isolation kit II following the manufacturer's instructions. The purity of $CD4^+$ T cells as determined by flow cytometry was 90−92%. For allogeneic T cell suppression studies, C57BL/6 DCs were co-incubated with the VD_3 MP + TGF-β1 MP combination or relevant soluble and MP control treatments in 96-well tissue culture plates for 48 h at 37 °C in culture media (RPMI 1640 with L-glutamine (Lonza, Walkersville, MD), 10% fetal bovine serum (Hyclone, GE Healthcare Life Sciences, Marlborough, MA), and 1% penicillin−streptomycin (Lonza)). Free MPs were washed as above, followed by addition of Balb/c $CD4^+$ T cells (150 000 Balb/c T cells:25 000 C57BL/6 DCs). They were added to each well and incubated at 37 °C for 3 days. Bromodeoxyuridine (BrdU) (Becton Dickinson) was pulsed into the culture media for the last 4 h. T cells were then stained for BrdU according to manufacturer's specifications. Allogeneic T cell proliferation and Treg differentiation were quantified by flow cytometry.

DOI: 10.1021/acsbiomaterials.9b00332
ACS Biomater. Sci. Eng. 2019, 5, 2631−2646

2.5. Microparticle Trafficking. Microparticle uptake and trafficking to secondary lymphoid organs were assessed by immunohistochemistry and flow cytometry. Phagocytosable MPs were concomitantly loaded with VD_3 or insulin and Vybrant DiI (Invitrogen, Carlsbad, CA) fluorescent labeling dye by adding 100 μL of DiI directly into the oil phase at 1 mg/mL in methanol per 500 mg of PLGA MPs. Nondrug loaded (unloaded) phagocytostable fluorescent MPs were also fabricated. Large, nonphagocytosable MPs (TGF-β1, GM-CSF, or unloaded) were fabricated in the standard fashion without the addition of fluorescent dye. 8- to 12-week-old female NOD mice were injected subcutaneously in the right upper abdominal region, anatomically proximal to the pancreas, with 10 mg of MP total (1:1:1:1 MP mass ratio; 2.5 mg of each of the four drug-loaded MP) in 0.2 mL of PBS. Secondary lymphoid organs were excised 48 h later and processed for immunohistochemistry (IHC) or flow cytometry

For IHC, axillary lymph nodes (ALNs) were first fixed in 3.2% paraformaldehyde at 4 °C for 24 h and then cryoprotected in 30% sucrose at 4 °C for 24 h, embedded in OCT (Sakura Finetek, Torrance, CA), and flash frozen. 15 μm sections were cut, air-dried for 30 min at RT, washed 3× in PBS, and blocked for 1 h at RT with 10% normal goat serum (Sigma-Aldrich) in wash solution (0.3% Triton-X-100 in PBS). Primary antibodies were incubated overnight at 4 °C at 1:100 dilution in wash solution containing 1% normal goat serum. Samples were washed 3× in wash solution, followed by incubation with secondary antibodies at 1:250 dilution in wash solution for 1 h at RT. Lastly, samples were washed 3× in wash solution and mounted with ProLong gold antifade mountant (Thermo Fisher Scientific). Sections were analyzed on a Zeiss LSM 710 confocal microscope (Carl Zeiss AG, Oberkochen, Germany). For flow cytometry, cells were isolated from dLNs proximal to the injection site (ALNs and inguinal LNs (ILNs)) and spleen and stained with primary conjugated antibodies as described below. Cells from naïve, non-MP injected NOD mice were included as controls.

2.6. In Vivo Imaging of Fluorescent Microparticles. Microparticles encapsulating immunomodulatory agents were prepared as described above but also with the inclusion of infrared dyes for visualization of the MPs in vivo. Phagocytosable MPs were concomitantly loaded with VD_3 or insulin and IRDye 800RS (745 nm excitation, 800 nm emission; LI-COR Biosciences, Lincoln, NE, USA), and nonphagocytosable MPs were concomitantly loaded with TGF-β1 or GM-CSF and IRDye 700DX (640 nm excitation, 700 nm emission; LI-COR). Infrared dyes were incorporated directly to the oil phase in MP fabrication by adding 100 μL at 1 mg/mL in methanol per 500 mg of PLGA MPs

Balb/c mice were fed an alfalfa-free diet for 2 weeks prior to imaging, per manufacturer's recommendations (LI-COR Biosciences) as certain grain sources can contribute to fluorescent background in near-infrared channels.[41] Subsequently, mice were subcutaneously injected in the abdominal region with 10 mg of MP total (1:1:1:1 MP mass ratio; 2.5 mg of each of the four drug-loaded MP) in 0.2 mL of PBS. At 3, 24, 48, and 72 h after injection, animals were anesthetized and scanned using the PerkinElmer (Caliper) IVIS Spectrum in vivo system. Utilizing the Living Image Analysis software, regions of interests (ROIs) were drawn around areas exhibiting fluorescence and the total radiant efficiency within the ROI was used for subsequent quantitative analysis.

2.7. Diabetes Prevention. Eight-week-old female NOD mice were randomized into eight treatment groups (n = 10/group) as follows: (1) unloaded MPs only; (2) GM-CSF MPs + insulin MPs; (3) TGF-β1 MPs + insulin MPs; (4) VD_3 MPs + insulin MPs; (5) dMP (VD_3 MPs + TGF-β1 MPs + GM-CSF MPs + insulin MPs); (6) insulin MPs; (7) VD_3 MPs + TGF-β1 MPs + GM-CSF MPs; (8) soluble equivalent bolus of encapsulated drugs (VD_3,TGF-β1, GM-CSF, insulin). Animals were injected with the described formulations once per week for the first 3 weeks (8, 9, and 10 weeks of age) subcutaneously in the right upper abdominal region, anatomically proximal to the pancreas, and given a booster once monthly thereafter for 4 months (12, 16, 20, and 24 weeks of age). All MP injections consisted of 10 mg of MPs (1:1:1:1 MP mass ratio) in 0.2 mL of PBS. Unloaded MPs were added to control formulations where there was an omitted factor, in order to deliver equivalent PLGA MP mass across group. Blood glucose levels were monitored once weekly for 20 weeks, and diabetes onset was defined as blood glucose levels of ≥240 mg/dL for 2 consecutive days.

An additional cohort of mice (excluded from Kaplan−Meier survival analysis) was evaluated at cross-sectional time points (10, 12, and 14 weeks of age). For the animals analyzed on week 12, mice were sacrificed prior to injection of the week 12 booster. Draining LNs, pancreatic lymph nodes (pLNs), and spleen were harvested and analyzed by flow cytometry to interrogate cellular phenotypes as potential mechanisms of therapy.

2.8. Diabetes Reversal. A cohort of female NOD mice were screened for hyperglycemia 3× per week beginning at 12 weeks of age. Newly diabetic mice (i.e., blood glucose levels of ≥240 mg/dL for 2 consecutive days) between 12 and 28 weeks old were implanted with an insulin pellet containing subcutaneously in the scruff that contained 13 mg of insulin for continuous release of 0.1 unit/24 h (LinShin Canada, Inc.) to temporarily restore normoglycemia. Mice were serially enrolled into the following treatment groups: (1) untreated (insulin pellet only); (2) dMP (VD_3 MPs + TGF-β1 MPs + GM-CSF MPs + insulin MPs); (3) soluble equivalent bolus of encapsulated drugs (VD_3, TGF-β1, GM-CSF, insulin) + unloaded MPs. Treatment began on the day of diabetes onset, and each group received three MP injections in the first week (days 0, 3, and 6) followed by three weekly booster injections (days 13, 20, and 27). Blood glucose levels were monitored twice weekly for 100 days, and mice were removed from the study when blood glucose reached ≥400 mg/dL on consecutive days.

2.9. Microparticle Pyrogenicity. Pyrogenicity of the MP vaccine formulation was evaluated via a rabbit pyrogen test, as specified in USP XXII, 1990 Monograph 151, "Pyrogen Test". This study was performed by the Bioreliance Corporation (Rockville, MD). Briefly, an amount of 5 mg of each MP type was combined and reconstituted in sterile PBS prior to injection into the ear vein of healthy, mature rabbits. Following injection, rectal body temperature of the rabbits was recorded over the course of 3 h where temperature fluctuation indicates pyrogenicity.

2.10. Cell Staining and Antibodies. For experiments involving flow cytometry (sections 2.3, 2.4, 2.5, and 2.7), a general staining protocol was utilized as follows: (1) cells were isolated into a single cell suspension and stained with fixable viability dye (Green or Near-IR; Life Technologies) for 10 min at RT, (2) washed and blocked with anti-CD16/32 (FCγ III/II receptor, clone 2.4G2, Thermo Fisher Scientific) for 15 min on ice, (3) fluorescent conjugated and/or primary antibodies incubated at a 1:100 to 1:250 dilution for 30 min on ice, (4) washed and data immediately acquired or fixed with paraformaldehyde for future acquisition. If intracellular staining was required, cells were washed and fixed/permeabilized after step 3 with Intracellular Fixation and Permeabilization Buffer Set (eBioscience) according to the manufacturer's instructions, and intracellular markers were stained with fluorescent conjugated and/or primary antibodies. Data were collected on a LSR II (BD Biosciences) or a Guava Easycyte flow cytometer (Millipore Sigma) and analyzed with either FlowJo software (Tree Star, Ashland, OR) or FCS Express 5 (De Novo Software, Glendale, CA).

Cells were stained with the following antibodies: anti-CD11c (BD Biosciences, PE-Cy7, clone N418), anti-CD11c (Biolegend, BV605, BV650, clone N418), anti-CD80 (BD Biosciences, APC, clone 16-10A1), anti-CD86 (BD Biosciences, FITC, clone GL1), anti-MHC Class II (I-A/I-E) (eBioscience, PE, clone M5/114.15.2), anti-FoxP3 (eBioscience, PE, clone FJK-16s), anti-CD25 (BD Biosciences, FITC, clone 7D4), anti-CD45 (Biolegend, APC-Cy7, clone 30-F11), anti-PD-L1 (Biolgened, BV421, clone 10F.9G2), anti-BTLA (BD Biosciences, BV711, clone HMBT-6B2), anti-CD4 (Biolegend, APC, clone RM4-5), anti-CD3 (Biolegend, Pacific Blue, clone 17A2), anti-CD8 (Biolegend, BV711, clone 53-6.7), anti-PD-1 (Biolegend, PE, clone 29F.1A12), anti-CD11b (Biolegend, APC, clone M1/70). Primary antibodies (not fluorescently conjugated) were used to detect CD3e (polyclonal; BD Biosciences), anti-IDO

DOI: 10.1021/acsbiomaterials.9b00332
ACS Biomater. Sci. Eng. 2019, 5, 2631−2646

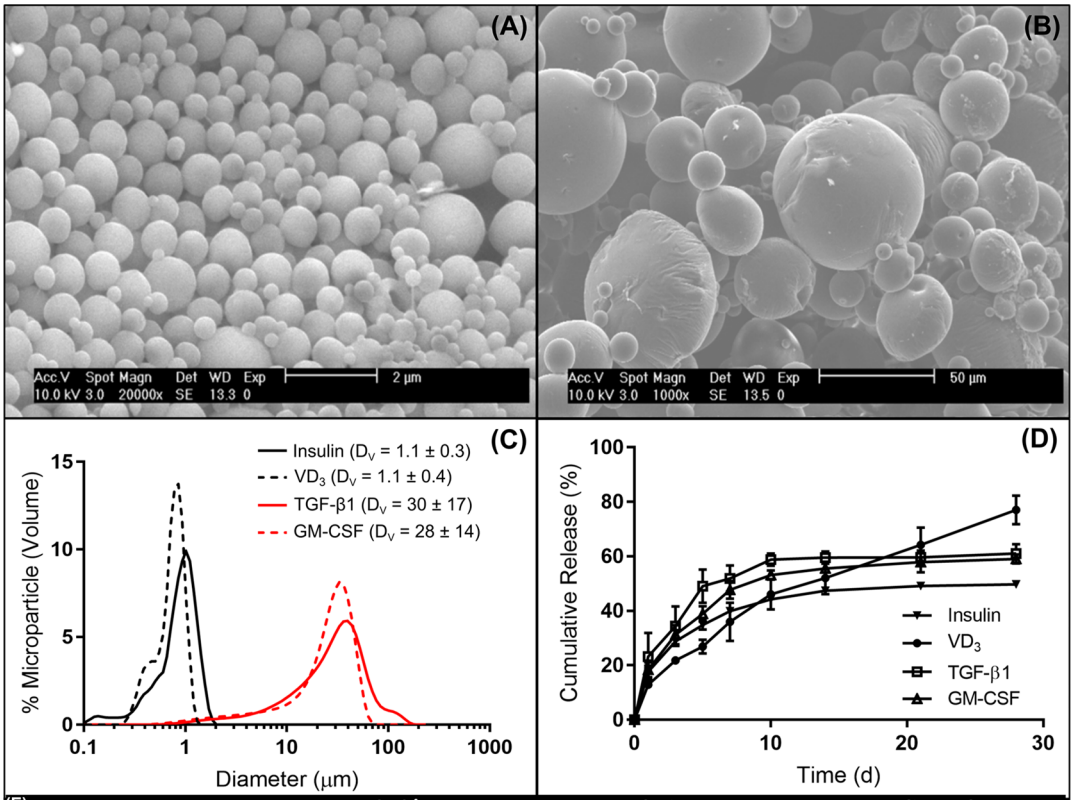

(E)

Encapsulated Agent	Mass Loaded/PLGA (μg/100 mg)	Encapsulation Efficiency ± SD (%)	Mass Delivered per Injection ± SD (ng)
Denatured Insulin	2580	10 ± 1	6,400 ± 450
Vitamin D_3	10	66 ± 3	165 ± 10
TGF-β1	5	61 ± 5	75 ± 5
GM-CSF	8	66 ± 4	130 ± 10

Figure 2. Characterization of fabricated microparticles. Representative SEM images of (A) phagocytsoable MPs and (B) nonphagocytosable MPs show size and surface morphology. (C) Size distributions of phagocytosable MPs (vitamin D_3 or insulin) and nonphagocytosable MPs (TGF-β1 or GM-CSF) were confirmed by dynamic light scattering, reporting mean and standard deviation in the legend (n = 5). (D) Release kinetics of encapsulated factors from biodegradable PLGA MPs over 28 days, as determined by ELISA or spectrophotometry (n = 3−5). (E) The loading efficiencies of encapsulated agents and mass delivered per 2.5 mg of PLGA injection is calculated. Data are represented by the mean ± SEM.

(Millipore, purified, clone 10.1), and B220 (polyclonal; BD Biosciences). Secondary antibodies included anti-rat IgG (Alexa Fluor 488; Invitrogen) and anti-hamster IgG (Alexa Fluor 594; Invitrogen).

2.11. Statistical Analysis. GraphPad Prism version 7 software (GraphPad Software, La Jolla, CA) was used for all statistical analyses. Unpaired t test, one-way ANOVA, one-way repeated measures ANOVA, Pearson's χ^2 test, and Kaplan−Meier estimator were applied as indicated. Bonferroni's, Tukey's, and Dunnett's post hoc tests were used to account for multiple comparisons as indicated. Data are presented as the mean ± SEM, with P values of ≤0.05 considered significant.

3. RESULTS

3.1. Microparticle Fabrication and Characterization. A previous formulation of the dMP platform established the efficacy of this combinatorial dMP platform to prevent diabetes in 4-week-old NOD mice.[31] At 4 weeks of age, NOD mice are prediabetic and display minimal insulitis with the majority of islets devoid of leukocyte infiltration.[42] By 8 weeks of age, in contrast, NOD mice typically remain prediabetic but exhibit significant β-cell loss and T cell infiltration in pancreatic islets.[42,43] When the previous dMP formulation was administered to 8-week-old NOD mice, preventative efficacy of the dMP was not realized (Figure S1). In order to enhance the applicability, the dMP formulation was modified to increase loading of chemotactic and tolerogenic factors. Furthermore, the insulin B_{9-23} peptide, previously used as the autoantigen, was replaced with denatured whole insulin. This decision was made to account for the possibility of epitope spreading, a process that describes the expansion of the autoantigen repertoire as pancreatic tissue damage releases neoantigens, an established phenomenon in NOD mice as disease progresses.[44] Insulin was denatured by heat and chemically by 2-mercaptoethanol as to not be nonmetabolically active. Single-agent MPs were each loaded with one of the four factors (GM-CSF, TGF-β1, VD_3, and insulin) individually using single- or double-emulsion solvent evaporation techniques as dictated by the solubility of the factors. Microparticles were characterized by SEM, sized by dynamic light scattering, and loading and release kinetics were determined (Figure 2). Scanning electron microscopy images demonstrated that surface morphology of each size of MP was spherical and smooth (Figure 2A,B). The diameters of the large, nonphagocytosable MPs containing GM-CSF or TGF-β1 were consistently found to be ∼30 μm, while small MPs containing VD_3 or insulin were ∼1 μm in diameter (Figure 2C),

DOI: 10.1021/acsbiomaterials.9b00332
ACS Biomater. Sci. Eng. 2019, 5, 2631−2646

appropriately sized for phagocytosis. Encapsulation efficiency of the loaded factors was >60% for the chemotactic and tolerogenic factors, while insulin loading efficiency was ~10% (Figure 2E), reflective of the high loading concentration used. In comparison to our previous dMP formulation for T1D prevention (Figure S1 and ref 31), administration of the updated formulation resulted in 5.1-fold, 2.6-fold, and 1.6-fold increase in TGF-β1, GM-CSF, and VD_3 delivered per injection, respectively. Release kinetics of the encapsulated drugs in PLGA MPs showed initial burst release followed by sustained release over 2−4 weeks (Figure 2D).

3.2. Microparticles Induce Suppressive DCs in Vitro. The ability of these MPs to drive a suppressive phenotype in murine bone marrow-derived DCs was assessed in vitro (Figure 3). In comparison to the negative control of untreated immature DCs (iDC), MHC-II$^+$ cell frequencies were significantly lower in DCs treated with VD_3 MPs or upon incubation with a combination of VD_3 MPs and TGF-β1 MPs (Figure 3A; representative flow analysis Figure S2A). Similarly, frequency of CD80$^+$ DCs decreased upon exposure to either TGF-β1 MPs or a combination of VD_3 MPs and TGF-β1 MPs. Levels of CD86 expression similar to iDCs were maintained by the combination of VD_3 MPs and TGF-β1 MPs. Note that GM-CSF MPs were not included in this in vitro analysis because GM-CSF is required in media to maintain bone-marrow derived DCs in culture. Unloaded PLGA MPs slightly increased the frequency of DCs expressing both CD80 and MHC-II, whereas a positive control of LPS stimulation dramatically increased all three surface markers. Of the MP-treated DCs, only the combination of VD_3 MPs and TGF-β1 MPs resulted in concomitant reduction of CD80$^+$ and MHC-II$^+$ DCs. Equivalent soluble doses of MP-encapsulated factors VD_3 and TGF-β1 (as determined by loading and release kinetics from Figure 2) were incubated with DCs to evaluate the impact of PLGA MP-based delivery on surface expression of maturation markers (Figure S3A). Compared to soluble factor delivery, microparticle encapsulation of TGF-β1 did not influence the relative surface expression of CD80, CD86, or MHC-II on DCs. On the other hand, encapsulation of VD_3 in phagocytosable MPs diminished the frequency of CD86$^+$ or MHC-II$^+$ DCs when compared to addition of soluble VD_3. In contrast, compared to equivalent soluble doses, the combination of VD_3 MPs and TGF-β1 MPs increased the frequency of CD86$^+$ or MHC-II$^+$ DCs but decreased the relative frequency of CD80$^+$ DCs.

Resistance to LPS maturation was investigated to determine the extent to which DCs pretreated with immunomodulatory MPs were programmed to be refractory to inflammatory stimulus (Figure 3B; representative flow analysis Figure S2B). Dendritic cells incubated with VD_3 MPs or TGF-β1 MPs alone both showed resistance to LPS maturation, as the percentage of cells expressing CD86 was diminished compared to LPS-stimulated DCs. Similar to culture without LPS, only DCs treated with the combination of VD_3MPs and TGF-β1 MPs decreased populations compared to LPS activation for two markers (CD86$^+$ and MHC-II$^+$), although CD80 frequency was not reduced. Media supplementation with equivalent soluble concentrations of VD_3 or TGF-β1 did not generally alter DC surface expression compared to MP delivery (Figure S3B). The only difference observed was that VD_3 MPs reduced the percentage of cells expressing CD86 relative to treatment with soluble VD_3.

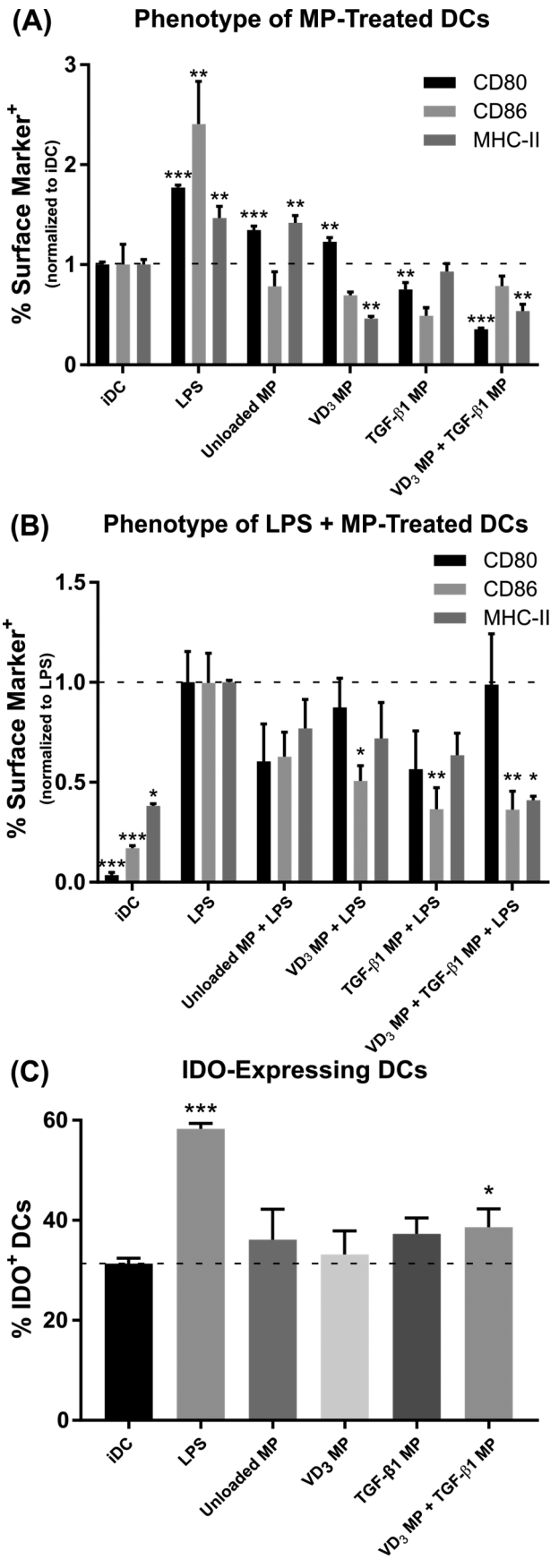

Figure 3. Co-incubation of vitamin D_3(VD_3) MPs and TGF-β1 MPs induce DCs with suppressive phenotypes in vitro. Dendritic cells were incubated with 10 mg of nonphagocytosable TGF-β1 MPs, and

DOI: 10.1021/acsbiomaterials.9b00332
ACS Biomater. Sci. Eng. 2019, 5, 2631−2646

Figure 3. continued

phagocytosable VD_3 MPs were added at a 10:1 MP to DC ratio. Microparticles were incubated with bone marrow-derived DCs for 48 h and subsequently washed with PBS to remove MPs. Untreated, immature DCs (iDC), DCs stimulated with LPS (1 μg/mL), and DCs incubated with unloaded MPs were included as controls. (A) Maturation markers CD80, CD86, and MHC-II were characterized by flow cytometry on MP-treated DCs and controls (n = 3). Surface expression is normalized to iDCs. (B) Maturation resistance in response to LPS was quantified (n = 3). Dendritic cells were stimulated with LPS (1 μg/mL) for 24 h following MP treatment. Flow cytometric analysis quantified expression of CD80, CD86, and MHC-II. Surface expression is normalized to LPS stimulated DCs. (C) Dendritic cell expression of the immunosuppressive enzyme IDO was quantified in response to MP treatment (n = 3). P-values (∗ = ≤0.05, ∗∗ = ≤0.01, ∗∗∗ = ≤0.001) were obtained by one-way ANOVA with Dunnett's multiple comparisons test against the iDC control (A, C) or the LPS-stimulated control (B). Data are represented by the mean ± SEM.

In addition to positive stimulatory markers, we measured DC expression of indoleamine 2, 3-dioxygenase (IDO) (Figure 3C; representative flow analysis Figure S2C), a powerful immunoregulatory enzyme that catalyzes the degradation of the essential amino acid tryptophan into kynurenine.[45] Among untreated iDCs, nearly 30% stained positive for IDO. As expected, IDO expression doubled in response to LPS stimulation, which has been shown to serve as regulatory response to limit deleterious inflammation in DCs.[46] Interestingly, of the MP treatment groups, only the combination of VD_3 MPs and TGF-β1 MPs significantly increased the frequency of IDO^+ DCs to 39%, above the 31% observed for the iDC group, although it is unclear what role an increase of this magnitude may play. Addition of equivalent soluble doses of VD_3 or TGF-β1 was not as effective at inducing IDO expression in DCs (Figure S3C), but the combination of soluble factors was comparable to VD_3 MP and TGF-β1 MP-treated DCs.

3.3. Microparticle-Treated DCs Suppress T Cell Proliferation and Induce Tregs. To determine the suppressive capacity of the dMP-generated DCs in vitro, proliferation of allogeneic splenic $CD4^+$ T cells in response to MHC mismatched DCs in a mixed lymphocyte reaction assay was quantified by incorporation of the synthetic nucleoside bromodeoxyuridine (BrdU) (Figure 4). Specifically, 17% of Balb/c T cells proliferated when cultured with C57Bl/6 iDCs, while in comparison, pretreatment of DCs with unloaded MPs suppressed T cell proliferation to 9% (Figure 4A; representative flow analysis Figure S4A). Proliferation was further reduced in groups where DCs were treated with VD_3 MPs or TGF-β1 MPs (<5%), with only VD_3 MPs or the combination of MPs diminishing allogeneic T cell proliferation to levels comparable with T cell only controls (<2%). Dendritic cells pretreated with soluble boluses of suppressive factors were not as effective at reducing T cell proliferation when compared to MP-encapsulated equivalent doses (Figure S3D). Coculture with DCs pretreated with soluble VD_3, TGF-β1, or a combination of the two resulted in 5%, 10%, and 2% of T cells proliferating, respectively. In contrast, treatment with MPs encapsulating equivalent doses diminished T cell proliferation to 2%, 3%, and 1%, respectively.

Conversion of T cells to a regulatory $CD25^+FoxP3^+$ Treg phenotype was also quantified after allogeneic coculture

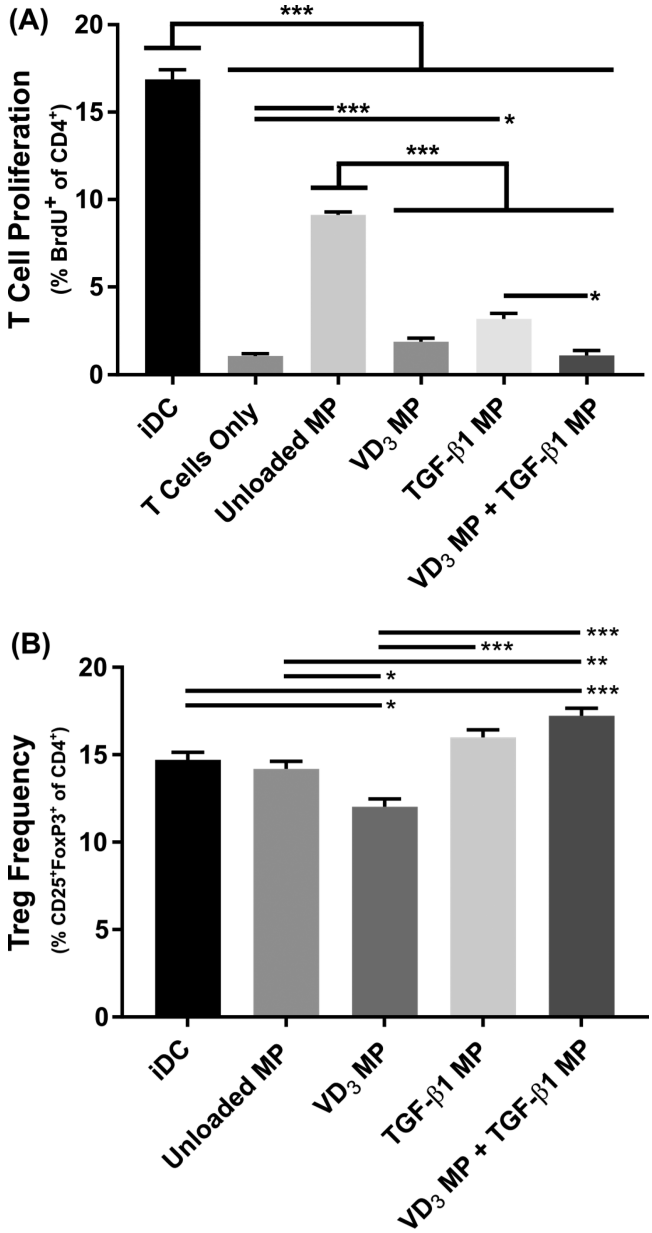

Figure 4. Co-incubation of vitamin D_3 (VD_3) MPs and TGF-β1 MPs generates suppressive DCs that inhibit proliferation of allogeneic T cells and induces a modestly higher Treg frequency in vitro. Dendritic cells were incubated with 10 mg of nonphagocytosable TGF-β1 MPs, and phagocytosable VD_3 MPs were added at a 10:1 MP to DC ratio. Microparticles were incubated with DCs for 48 h and subsequently washed with PBS to remove MPs. Balb/c splenic $CD4^+$ T cells were then added to the MP-treated C57Bl/6 bone marrow-derived DCs at a 150 000:25 000 ratio. Untreated, immature DCs (iDC) and T cells only were included as controls. After 72 h, flow cytometry assessed T cell proliferation via BrdU incorporation (A) and $CD25^+FoxP3^+$ Treg frequency (B) (n = 3). P-values (∗ = ≤0.05, ∗∗ = ≤0.01, ∗∗∗ = ≤0.001) were obtained by one-way ANOVA with Tukey's significance test. Data are represented by the mean ± SEM.

(Figure 4B; representative flow analysis Figure S4B). Coculture of T cells with DCs treated with TGF-β1 MPs or unloaded PLGA MPs did not influence conversion or expansion of Tregs. Alternatively, VD_3 MP-treated DCs decreased the frequency of Tregs compared to untreated iDCs, diminishing Treg prevalence from 15% to 12% of total

DOI: 10.1021/acsbiomaterials.9b00332
ACS Biomater. Sci. Eng. 2019, 5, 2631−2646

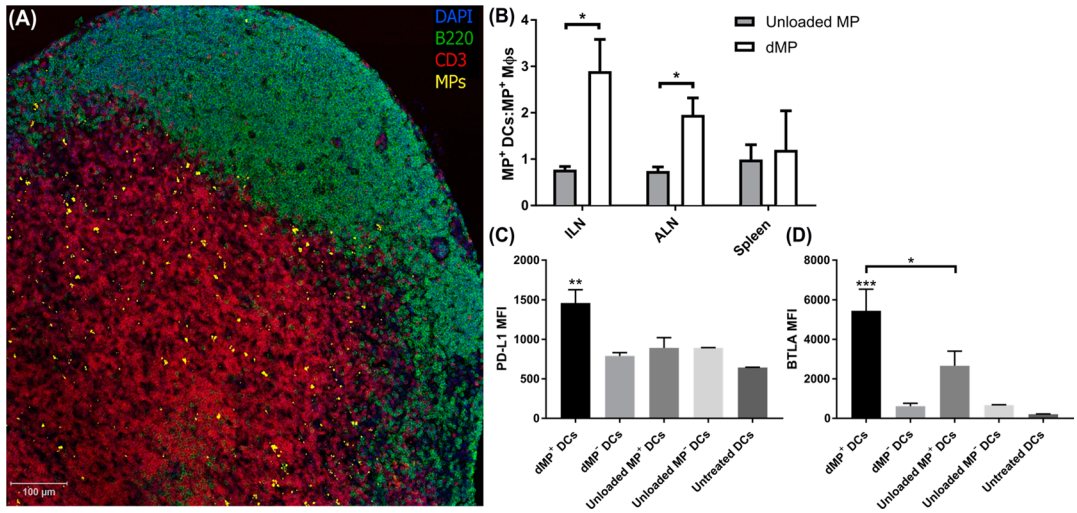

Figure 5. Subcutaneously injected MPs traffic to lymph nodes primarily by DCs with a suppressive phenotype in vivo. NOD mice were subcutaneously injected in the abdominal region with either the dMP or unloaded MPs. Encapsulated agents (VD_3, insulin, or unloaded) in phagocytosable MPs were concomitantly loaded with fluorescent dye (DiI). (A) Axillary lymph nodes (ALN) were excised 48 h after dMP administration, and IHC was performed to identify MP localization. (B) Lymphoid organs (ALN, inguinal lymph nodes (ILN), and spleen) were excised from NOD mice 48 h after subcutaneous MP injection and cells characterized by flow cytometry for MP presence. The ratio of MP^+ frequency in $CD11b^+CD11c^+$ DCs relative to $CD11b^+CD11c^-$ MΦs was assessed and compared to unloaded MP-treated mice ($n = 3–4$). (C, D) PD-L1 and BTLA mean fluorescent intensity (MFI) was evaluated in ALNs on dMP^+ DCs, dMP^- DCs, unloaded MP^+ DCs, unloaded MP^- DCs, and DCs from untreated mice ($n = 3–4$). *P*-values (∗ = ≤0.05, ∗∗ = ≤0.01, ∗∗∗ = ≤0.001) were obtained by two-tailed unpaired Student's *t* tests (B) and one-way ANOVA (C, D) with Tukey's significance test. Data are represented by the mean ± SEM.

$CD4^+$ T cells. Only the combination of VD_3 MPs and TGF-β1 MP-treated DCs increased Treg frequency compared to iDCs, resulting in a modest increase of Tregs from 15% to 17%. In contrast to previous results which generally showed MP encapsulation augmented immunomodulation, pretreatment with VD_3 MPs or TGF-β1 MP somewhat decreased Treg frequency when compared to soluble equivalent doses of VD_3 or TGF-β1 (Figure S3E). In contrast, Treg frequencies for the combination treatments were comparable between VD_3 MP and TGF-β1 MP-treated DCs and the soluble VD_3 and TGF-β1-treated DCs.

3.4. Subcutaneously Injected MPs Drain to Lymph Nodes, Are Localized Primarily in DCs, and Induce a Suppressive Phenotype in Vivo. As a next step, MP trafficking was assessed in vivo to identify draining to peripheral LNs and to characterize the resultant phenotype of MP-bearing DCs (Figure 5). Agents in phagocytosable MPs (VD_3, insulin, or unloaded) were encapsulated alongside fluorescent dye to assist in delineating MP trafficking kinetics. Fluorescent PLGA MPs without bioactive factors (unloaded MPs) were fabricated as a comparison to identify the impact on delivery of the chemotactic and tolerogenic factors in the dMP. Female NOD mice were injected subcutaneously in the right upper abdominal region, anatomically proximal to the pancreas, with 10 mg of MP total (1:1:1:1 MP mass ratio; 2.5 mg of each of the four drug-loaded MP) in 0.2 mL of PBS. Two days after subcutaneous injection in NOD mice, fluorescent MPs were found in excised proximal dLNs (inguinal and axillary) (Figure 5A). As expected, MPs were primarily localized to the paracortex, a T-cell-rich zone where circulating APCs enter the node. We further evaluated MP trafficking by investigating the subset of phagocytic APCs associated with the fluorescent MPs in dLNs via flow cytometry. When compared to unloaded MP^+ cells, dMP^+ leukocytes in proximal dLNs were significantly more localized to DCs than macrophages (MΦs), depicted as the MP^+ DCs:MΦs ratio (Figure 5B; representative flow analysis Figure S5A,B). The ratio of dMP^+ DCs to dMP^+MΦs was consistently ≥1 throughout lymphoid organs and as high as ∼3:1 in the inguinal LNs, and in contrast, the ratio of unloaded MP^+DCs:MΦs was ∼1:1 in all lymphoid organs. Importantly, the suppressive phenotype of these DCs varied depending on the MP formulation administered. Inhibitory programmed death-ligand 1 (PD-L1) expression on dMP^+DCs was roughly 2-fold higher than dMP^-DCs, unloaded MP^+ DCs, unloaded MP^- DCs, and untreated DCs isolated from a naïve NOD mouse (Figure 5C; representative flow analysis Figure S5C). Similarly, surface expression of B and T lymphocyte attenuator (BTLA), a co-inhibitory receptor that was recently shown to be pivotal for DC-based induction of Tregs,[47] was substantially upregulated in dMP^+DCs compared to controls (Figure 5D; representative flow analysis Figure S5D). Unloaded MP^+ DCs also displayed higher expression of BTLA compared to MP^-DCs, however, at a level approximately half that of dMP^+DCs.

Additionally, in vivo imaging using fluorescently loaded phagocytosable MPs and a separate fluorophore for non-phagocytosable MPs showed that large, nonphagocytosable MPs persist at the site of injection whereas presence of small, phagocytosable MPs wanes over time (Figure S6). The total fluorescent signature of the nonphagocytosable MPs at the abdominal injection site did not significantly diminish over 72 h, as compared to fluorescence at the 3 h initial time point. In contrast, the fluorescent presence of phagocytosable MPs diminished rapidly, with an appreciable reduction in fluorescence at the site of injection within 24 h, consistent with phagocytic uptake and trafficking of the smaller MPs.

It was also observed that repeated administration of either dMP or unloaded MPs resulted in the formation of a palpable nodule at the subcutaneous injection site (Figure S7). Histological and flow cytometry analysis revealed high levels of proteinaceous deposition and leukocyte infiltration. The MP

DOI: 10.1021/acsbiomaterials.9b00332
ACS Biomater. Sci. Eng. 2019, 5, 2631−2646

depots comprised significant numbers of APCs, $CD4^+$, and $CD8^+$ T cells and small numbers of Tregs. The presence of a lymphatic endothelial marker, LYVE-1, was also found in dMP nodules. Notably, MP nodules resolved within 4 weeks of injection as determined by palpation and surgical examination.

3.5. dMP Administration Prevents T1D Onset in 8-Week-Old NOD Mice. We next investigated whether subcutaneous dMP injection could prevent diabetes onset in a mouse model of T1D (Figure 6). Late-stage T1D prevention was assessed in a cohort of eight-week-old, female prediabetic female NOD mice. Nonobese diabetic mice typically develop insulitis around 4−6 weeks of age and can exhibit hyperglycemia as early as 12 weeks old.[43] Animals were given three weekly injections beginning at 8 weeks of age followed by four monthly booster injections totaling seven treatments (at 8, 9, 10, 12, 16, 20, and 24 weeks of age). Eight treatment groups were included to assess the efficacy of the dMP (Figure S8). When accounting for all eight groups, statistical significance was not realized for the Kaplan−Meier survival analysis when accounting for multiple comparisons via Bonferroni correction, as the study was not powered to resolve this large number of groups. However, pairwise comparison between survival curves of mice that received the dMP and mice that received unloaded MPs resulted in a *P*-value of <0.05, suggesting a difference between treatments, which when corroborated with a fully powered diabetes reversal study (see Figure 8 and discussed below) and our previous report of the dMP in a mouse model of multiple sclerosis,[32] highlight trends of therapeutic efficacy when examined alongside the other treatment groups. Specifically, mice that received the dMP (VD_3 MPs + TGF-β1 MPs + GM-CSF MPs + insulin MPs) had reduced incidence of diabetes, with 60% of mice remaining nondiabetic at 28 weeks of age, as compared to 10% of mice that received unloaded MPs (Figure S8). In order to discuss results in a stepwise manner, isolated groups from Figure S8 were replotted to highlight specific features of the dMP (Figure 6). For example, administration of a soluble equivalent bolus of encapsulated drugs and antigen did not minimize disease incidence compared to unloaded MPs as a control, suggesting the dMP worked in a MP-encapsulation dependent manner (Figure 6A). Additionally, requirement of antigen as well as immunomodulatory capacity of the dMP platform was suggested as neither the dMP without insulin MPs nor insulin MPs alone halted diabetes onset (Figure 6B). Lastly, through treatment with individual immunomodulatory MPs and insulin MPs, results suggest that individually none of these factors are capable of providing the full therapeutic efficacy exhibited by the combination of factors in the dMP (Figure 6C).

3.6. dMP-Mediated T1D Prevention Is Associated with an Increase in Tregs, Upregulation of PD-1 on $CD4^+$ and $CD8^+$ T Cells, and an Increase in DCs in Draining Lymph Nodes. Cross-sectional flow cytometric analysis of dMP-treated NOD mice was performed to analyze markers of therapeutic mechanism associated with T1D prevention (Figure 7). Regulatory T cell frequencies were significantly increased in the spleen at all three time points examined (ages 10, 12, and 14 weeks old) and in the pancreatic LNs at ages 12 and 14 weeks old from dMP-treated mice as compared to untreated and unloaded MP treated groups (Figure 7A; representative flow analysis Figure S9A), indicating the PLGA alone was not responsible for the immunomodulatory effects seen. Draining ipsilateral LNs (inguinal + axillary) isolated from 12-week-old NOD mice

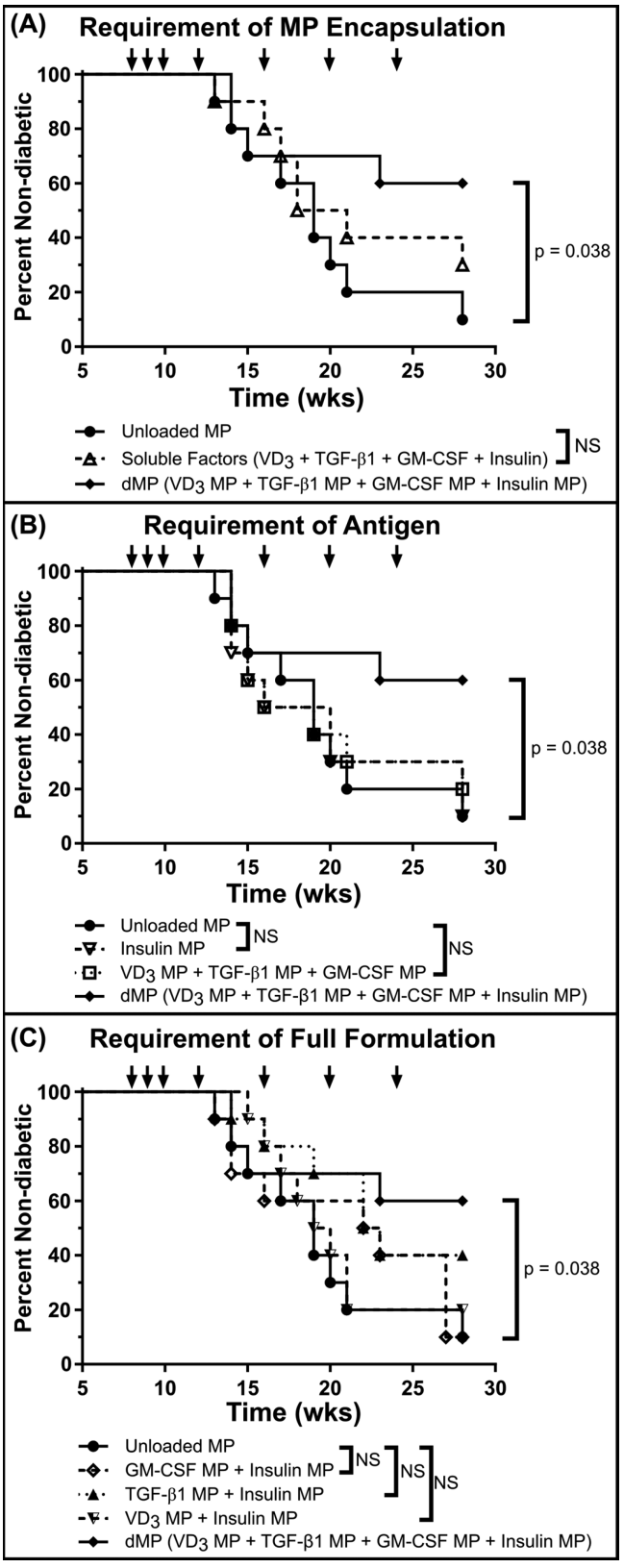

Figure 6. dMP administration prevents diabetes onset in NOD mice. A cohort of 8-week-old NOD mice (n = 10/group) were injected at a subcutaneous site anatomically proximal to the pancreas with the described MP formulations over 16 weeks. Animals received MP injections (arrows) once a week for the first 3 weeks (8, 9, and 10 weeks of age) and a booster injection once monthly thereafter for 4 months (12, 16, 20, and 24 weeks of age). Unloaded MPs, a soluble

DOI: 10.1021/acsbiomaterials.9b00332
ACS Biomater. Sci. Eng. 2019, 5, 2631−2646

Figure 6. continued

bolus of factors without MPs, and omission of factors were investigated. When a factor-loaded MP was omitted, unloaded MPs were delivered to deliver an equivalent PLGA mass. Animals were monitored weekly until week 28, and mice were considered diabetic when blood glucose levels were ≥240 mg/dL on 2 consecutive days. The full dMP (solid line with solid tilted square, VD_3/TGF-β1/GM-CSF/insulin MPs) and unloaded MPs groups were replotted alongside different experimental groups to highlight the requirement of MP encapsulation (A), antigen (B), and the full dMP formulation (C) in order to see maximum therapeutic effect. Survival data are fit using the Kaplan−Meier nonparametric survival analysis model, and statistical analysis was performed via log-rank test (Mantel−Cox method). Statistical significance was not realized when accounting for multiple comparisons via Bonferroni correction, as the study was not powered to resolve this large number of groups. However, pairwise comparison between survival curves of mice that received the dMP and mice that received unloaded MPs resulted in a *P*-value of <0.05, suggesting a difference between treatments.

also displayed upregulation of PD-1 on both $CD4^+$ and $CD8^+$ T cells (Figure 7B; representative flow analysis Figure S9B). Interestingly, this increased expression of PD-1 surface expression was only found on T cells in proximal dLNs (inguinal and axillary) and not in distal lymphoid organs (pancreatic LNs and spleen). In this case, the response to the biomaterial alone, unloaded PLGA MPs, was small but existent, where PD-1 expression was elevated on T cells isolated from ipsilateral dLNs compared to T cells from the contralateral LNs (mice were injected subcutaneously in the abdominal region on the right side). Notably, the inclusion of bioactive factors in PLGA MPs including the potent DC chemoattractant, GM-CSF, increased the frequency of DCs found in ipsilateral dLNs by 2.5-fold over contralateral LNs from unloaded MP treated mice (Figure 7C; representative flow analysis Figure S9C). Pancreata were also excised from a small cohort of 12-week-old mice and stained with hematoxylin and eosin (H&E) to quantify insulitis (Figure S10). Frequency and severity of insulitis between treatment groups was not statistically significant at 12 weeks of age. This finding is consistent with recent reports supporting the notion that insulitis is highly variable, is present in only a modest proportion of islets, and has limited relation to disease duration.[48]

3.7. dMP Administration Reverses Diabetes in Recent-Onset NOD Mice for a Limited Time. Lastly, we sought to determine whether the dMP vaccine could reverse hyperglycemia in NOD mice, a more clinically translatable model (Figure 8). Upon diabetes onset, NOD mice were immediately enrolled into one of three treatment groups and given a sustained release insulin pellet to temporarily restore euglycemia. Diagnostic blood glucose levels and age at diabetes onset were well matched between groups. Three initial injections in the first week postdiabetes onset followed by three weekly booster injections significantly prolonged the duration of diabetes remission in dMP-treated mice (up to 100 d) as compared to soluble drugs and antigen plus unloaded MP (up to 34 d) or untreated (up to 45 d) groups. While reversal of diabetes was not sustained in dMP-treated mice, the normoglycemic window was significantly extended. This was demonstrated as 36% of dMP-treated mice remained euglycemic by day 60. In contrast, 100% of mice that either received no treatment or the control treatment relapsed to severe hyperglycemia by days 45 and 34, respectively.

3.8. Microparticles Are Nonpyrogenic. A pyrogenicity test was assessed in adult rabbits, wherein an amount of 5 mg of each MP type was reconstituted in sterile PBS and administered intravenously (Figure S11). Following injection, there were no detectable changes in body temperature in treated animals over 3 h.

4. DISCUSSION

Beyond exogenous insulin administration, there are limited therapeutic options for patients living with T1D. Recent clinical trials have explored monoclonal antibody immunotherapy, anti-thymocyte globulin, islet transplantation, and autologous stem cell transfusion to mixed results.[6−11] While initially promising, these approaches have failed to provide long-term insulin independence. In addition, these treatments can sometimes employ potent immunosuppressive regimens, which leave patients at increased risk for cancer and opportunistic infection. Antigen-specific immunotherapy has potential to elicit controlled immunomodulation without systemic immunosuppression. Here, we demonstrate that a dMP approach, delivering immunomodulatory and chemotactic factors as well as antigen, can skew both innate and adaptive immunity toward a suppressive state, generate robust prevention of T1D onset in a late-stage, preclinical diabetes NOD mouse model, and extend euglycemia in recent-onset diabetic NOD mice.

We previously demonstrated efficacy of an early formulation of this dMP system in prediabetic, 4-week-old NOD mice.[31] Building on our initial platform, we sought an improved formulation with efficacy in a more stringent model of T1D prevention using 8-week-old NOD mice as well as in a rigorous diabetes reversal model. The updated dMP formulation described here was first adjusted to incorporate whole, denatured insulin in place of insulin B_{9-23} peptide, the goal being to expand the antigen repertoire tolerized by the dMP and ward against epitope spreading, an established phenomenon in both the NOD mouse model and human T1D.[44,49] Furthermore, loading amounts of tolerogenic and chemotactic factors were adjusted to deliver higher doses. For example, the mass of GM-CSF delivered was increased 2.5-fold to 132 ng per injection, in part due to reports showing the dose-dependent response of DC recruitment demonstrated by Ali et al.[33] Here, we first demonstrated that MPs encapsulating protolerogenic agents, TGF-β1 and VD_3, generated DCs with immunoregulatory phenotypes. We found that only the combination of both tolerogenic factors resulted in DCs with diminished CD80 and MHC-II expression, capable of resisting LPS-driven maturation, as well as upregulated IDO production. Due the complex pathogenesis and heterogeneity of T1D, it has been suggested that combinatorial approaches may be advantageous in generating more robust immune tolerance.[50,51] In support of this notion, combinatorial approaches targeting multiple immune pathways simultaneously have recently seen success in other disease fields, such as metastatic melanoma where the coadministration of anti-PD-1 and anti-CTLA-4 monoclonal antibodies dramatically improved survival, more so than either therapy alone.[52,53] In our model of immune suppression, treatment with the combination of MPs was crucial in inducing the most robust immune response. Suppressive DCs generated from the combination of MPs suppressed allogeneic T cell proliferation and increased Treg

DOI: 10.1021/acsbiomaterials.9b00332
ACS Biomater. Sci. Eng. 2019, 5, 2631−2646

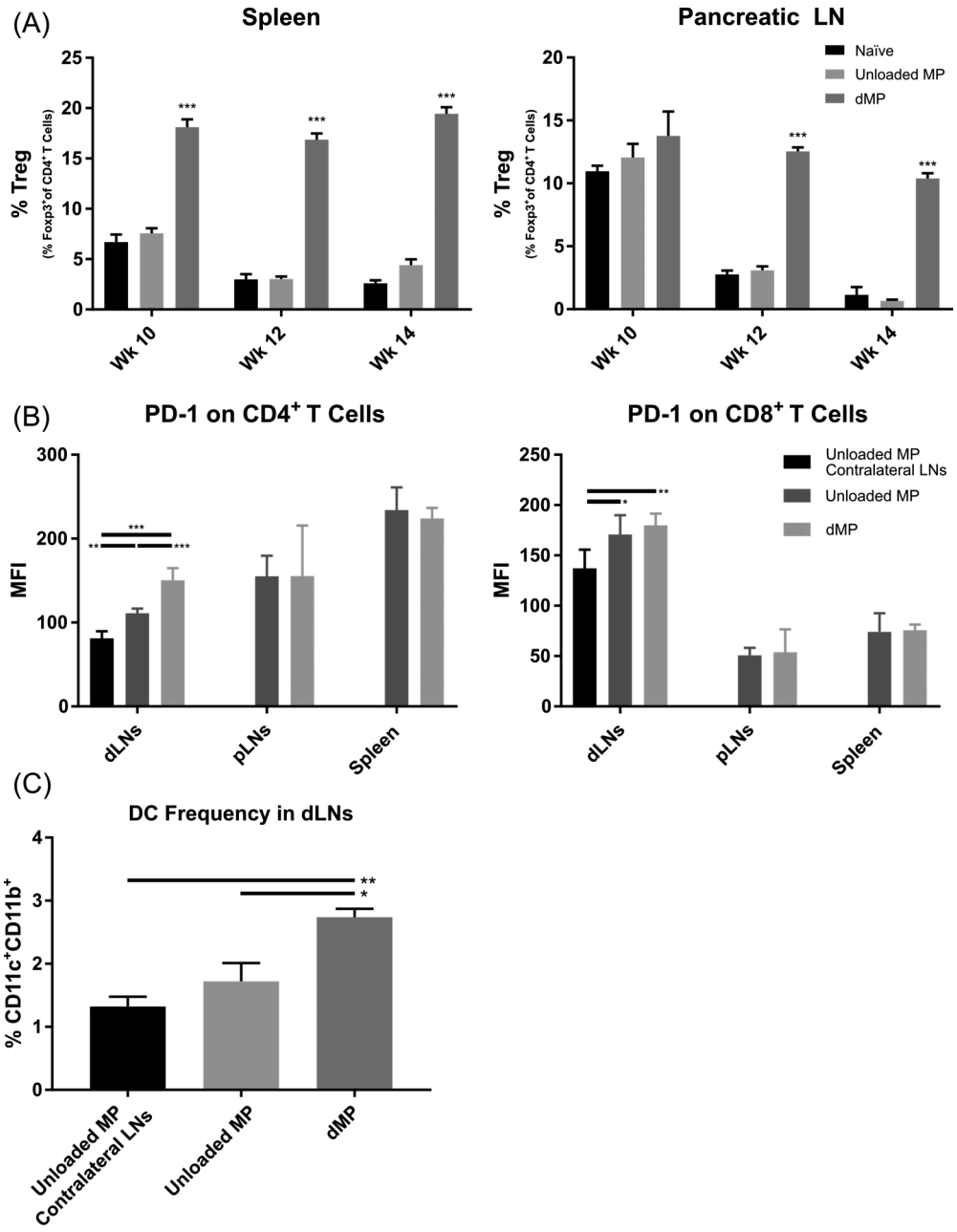

Figure 7. Diabetes prevention in dMP-treated mice is associated with an increase in Tregs, upregulation of PD-1 on $CD4^+$ and $CD8^+$ T cells, and an increase in DCs. Eight-week-old prediabetic NOD mice received MP injections at identical time points as in the prevention study and were euthanized at 10, 12, or 14 weeks of age. Mice analyzed at 12 weeks of age were sacrificed before receiving the week 12 monthly booster injection. As before, MP injections were administered subcutaneously on the right side of the abdomen, proximal to the pancreas. Ipsilateral inguinal and axillary LNs from dMP-treated mice and unloaded MP-treated mice were excised and stained for flow cytometry. Contralateral inguinal and axillary LNs from unloaded MP-treated mice were excised as a control. (A) Frequency of $FoxP3^+CD4^+$ T cells isolated from spleen and pancreatic LNs (pLNs) of 10-, 12-, and 14-week-old dMP-treated, unloaded MP-treated, and untreated naïve mice of total $CD4^+$ T cells was quantified (n = 5−6). (B) Lymphoid organs (draining lymph nodes (dLNs; combined axillary and inguinal LNs), pLNs, and spleen) from animals euthanized at 12 weeks of age were analyzed for PD-1 expression on both $CD4^+$ and $CD8^+$ T cells (n = 5). (C) Frequency of DCs in dLNs as a percent of total cells (n = 5). P-values (∗ = ≤0.05, ∗∗ = ≤0.01, ∗∗∗ = ≤0.001) were obtained by one-way ANOVA with Tukey's significance test. Data are represented by the mean ± SEM.

differentiation. We also showed that MP encapsulation of the tolerogenic agents, TGF-β1 and VD_3, was broadly more efficacious at generating suppressive DCs than equivalent soluble doses, highlighting the likely advantageous delivery of VD_3 to its nuclear receptor and controlled release aspects of the dMP system. In the context of T1D, these in vitro models suggest that dMP-treated DCs, which can encounter inflammatory signals released from the chronically inflamed pancreas, may be able to resist maturation.

Several recent particle-based immunotherapy reports have explored intra-LN injection to modulate immunity.[54−56] Here, we show that a simpler subcutaneous injection of our dMP vaccine results in trafficking of the phagocytosable MPs to dLNs, whereas nonphagocytosable MPs primarily remain at

DOI: 10.1021/acsbiomaterials.9b00332
ACS Biomater. Sci. Eng. 2019, 5, 2631−2646

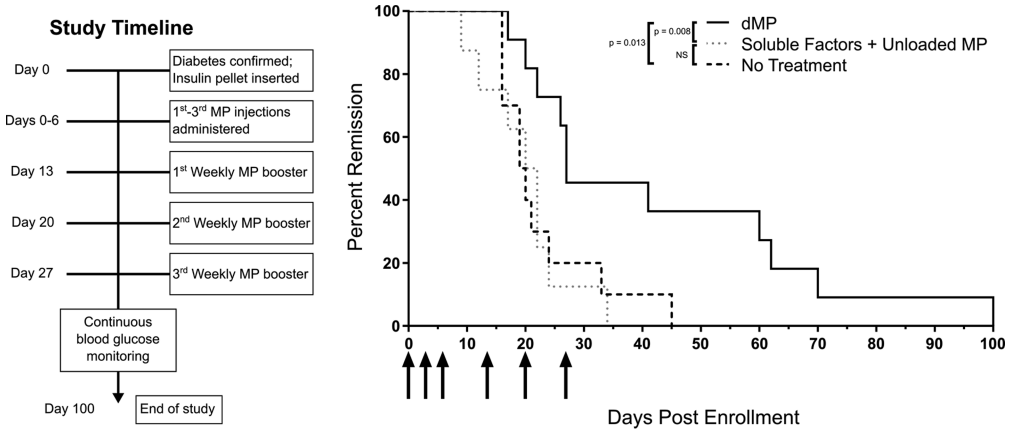

Figure 8. dMP administration in recent-onset NOD mice reverses T1D for a limited time period. Newly diabetic NOD mice (≥240 mg/dL on consecutive days) were serially enrolled in a recent-onset diabetes reversal study. Upon enrollment, animals received a sustained release insulin pellet to temporarily (∼2 weeks) control glycemia and immediately began MP treatment (left: study timeline). Mice received the dMP (n = 11), a soluble bolus of the four factors plus unloaded MPs (n = 8), or no treatment (n = 10) (right). Animals received MP injections (arrows) three times in the first week and three weekly booster injections. Blood glucose levels were monitored twice weekly, and mice were removed from the study upon diabetes recurrence. Survival data are fit using the Kaplan−Meier nonparametric survival analysis model, and statistical analysis was performed via log-rank test (Mantel−Cox method).

the site of injection. Fluorescently loaded phagocytosable MPs were shown to be primarily localized to the paracortex, suggesting interaction between the MP-bearing APCs and T cells. This is considered important due to the nature of T1D, which is a primarily T-cell-mediated, autoimmune disease. We also found that dMP administration localized MPs more to DCs than MΦs when compared to the trafficking patterns of unloaded MPs. This is advantageous and was a design criterion to include the potent DC chemokine GM-CSF because it is well established that DCs are the most effective APC in orchestrating the adaptive immune response. Microparticle-bearing DCs from dMP-treated mice also displayed suppressive hallmarks with upregulated expression of PD-L1 and BTLA. Fiorina and colleagues found that PD-L1 expression was diminished in NOD mice and human T1D patients and that genetically engineered overexpression of PD-L1 could inhibit disease onset.[57] Additionally, a recent report showing that ∼1% of cancer patients treated with anti-PD-1 or anti-PD-L1 checkpoint inhibitor therapy develop autoimmune T1D suggests that the converse, upregulation of PD-L1 is likely favorable for diabetes protection.[58] Similar beneficial effects of upregulating BTLA on DCs may be explained by recent work by Jones et al., which demonstrated a novel role of BTLA on the surface of DEC205$^+$CD8$^+$ DCs to be critically important for induction of Tregs.[47]

Subcutaneous injections of our dMP protected against diabetes onset in 60% of 8-week-old female NOD mice. While the study was not powered to detect differences when accounting for multiple comparisons via Bonferroni correction between the large number of controls investigated, only the full, four-factor dMP resulted in a pairwise significant difference between the unloaded PLGA MP treatment group. In contrast, treatment groups including the dMP without insulin MPs, a soluble equivalent bolus of encapsulated drugs and antigen, and the combination of MPs formulated with antigen and a single immunomodulatory factor did not prevent disease onset or demonstrate pairwise significance compared to unloaded MPs, suggesting the requirements of insulin antigen, the encapsulation of factors in PLGA MPs, and the delivery of all four MPs in order for the dMP to be maximally therapeutic. These trends of requiring MP encapsulation and disease-relevant antigen have been corroborated in our previous work on the dMP system which ameliorated MS in a mouse model,[32] in which we showed that an MS-specific dMP (with MS-specific antigenic peptide) inhibited autoimmunity, whereas a soluble equivalent bolus of encapsulated drugs and antigen or an irrelevant antigen dMP formulation (with ovalbumin peptide) both failed to mitigate disease.

While developing strategies to reverse existing T1D is desirable, therapies capable of preventing of delaying T1D with sufficient safety and tolerability are not only clinically relevant but perhaps even preferable due to the presence of functional endogenous β cell mass. This seems increasingly possible given current capability to stage presymptomatic T1D based upon genetic risk markers and measurements of autoantibodies in serum as well as dysglycemia.[59,60] Flow cytometry revealed that dMP-mediated prevention was associated with a systemic increase in Tregs, upregulation of PD-1 expression on CD4$^+$ and CD8$^+$ T cells, and an increase in DC frequency in dLNs, suggesting suppressive networks are induced to produce the observed T1D protection. The upregulation of PD-1 on CD8$^+$ T cells is noteworthy, as producing vaccines that direct CD8$^+$ T cell responses has historically proven difficult compared to modulating CD4$^+$ T cells.[61] As T1D pathogenesis is mediated by CD8$^+$ T cell destruction of pancreatic β-cells, a therapy capable of modulating cytotoxic T cells is highly desirable. Previous research has demonstrated that biodegradable MPs encapsulating antigen can promote prolonged antigen presentation and enhance the capacity for cross-presentation by nearly 1000-fold compared to soluble protein.[62] Furthermore, DCs are dramatically more efficient than MΦs at cross-presentation to CD8$^+$ T cells,[63] suggesting that the increase in dLN DCs and selective colocalization of dMPs with DCs versus MΦs could explain the responses measured.

In a mouse model of recent-onset T1D, we demonstrated that dMP administration could extend the window of euglycemia in dMP-treated mice compared to controls that received no treatment or a soluble bolus of the four drugs and unloaded MPs. While reversal was not sustained indefinitely, these results are comparable to similar platforms that do not

DOI: 10.1021/acsbiomaterials.9b00332
ACS Biomater. Sci. Eng. 2019, 5, 2631−2646

supplement immunotherapy with insulin therapy or islet transplantation. For example, daily treatment with IL-2 for 5 days after diabetes onset reversed T1D in ~40% of NOD mice by the eighth week after diagnosis with diabetes relapse increasing steadily over time, a similar percentage to our own therapy.[64] Incomplete reversal may be attributable to immunomodulation occurring at a time when insulin production may already be irrecoverable. Diabetes diagnosis in NOD mice arises at a time when an appreciable β-cell mass is destroyed or inactive, and little evidence suggests that endogenous β-cell regeneration or proliferation can naturally replace the lost capacity for insulin production,[65] although there are recent reports investigating new kinase-inhibitory drugs to induce β-cell proliferation,[66] which could be explored in conjunction.

Results of this study highlight the advantages of the dMP system compared to similar approaches. For example, previous reports of VD_3 or analogs to promote suppressive DCs and Tregs for T1D in vivo involved soluble administration, which relied on intraperitoneal injection every other day and also resulted in hypercalcemia.[67−69] In contrast, our controlled-release platform dramatically reduces dosing frequency and minimizes the drug load required due to localization and targeting to cells of interest. Similarly, researchers have demonstrated that ex vivo treatment of DCs with tolerogenic factors (VD_3 and VD_3 + dethamexasone, respectively) and loading of disease-specific antigen can mitigate autoimmunity in mouse models of MS and rheumatoid arthritis upon reinfusion.[70−72] However, this type of approach requires costly and potentially hazardous ex vivo manipulation of cells, which limits its clinical translatability. Other groups have attempted to generate antigen-specific tolerance using similar biomaterials concepts. In one approach, a T1D-specific peptide was coupled to a porous alginate hydrogel that contained gold NPs bearing GM-CSF.[73] While the authors show that the hydrogels resulted in substantial DC recruitment and modest antigen-specific Treg localization and proliferation, hydrogel administration had no significant impact on diabetes prevention in a comparable 8-week-old NOD cohort. In another report, Prasad et al. described how T1D-antigen-coupled splenocytes administered intravenously blocked diabetes onset in 5-week-old NOD mice at a rate comparable that seen in our studies.[74] When the authors moved to an antigen-coupled PLGA nanoparticle platform to avoid drawbacks of adoptive cell therapy, they saw similar results in antigen-defined adoptive transfer models of T1D (e.g., single T cell clone, precise number of $CD4^+$ T cells transferred, dearth of $CD8^+$ T cells and B cells). However, the authors did not investigate the antigen-coupled PLGA nanoparticles in preventing spontaneously occurring T1D in the poly-autoantigen NOD mouse model. Notably, their results demonstrated tolerance was at least in part maintained in a PD-1-dependent manner, similar to our finding. The same group has also previously reported that administration of MS-antigen-coupled splenocytes generated significant upregulation of PD-L1 on splenic marginal zone MΦs, highlighting the importance of the link between suppressive features on APCs and the resultant downstream T cell tolerance.[75]

5. CONCLUSIONS

These exciting results show that the dMP prevents and reverses T1D in an antigen-dependent manner, that localized controlled-release of these bioactive factors (insulin, VD_3, TGF-β1, GM-CSF) via biodegradable MPs is more effective than soluble administration, and that this combinatorial therapy works cooperatively to achieve greater immunomodulation than single immunomodulatory-factor MPs alone. Taken together with our recent report demonstrating the efficacy of this dMP platform in a mouse model of MS upon substitution to a MS-specific antigen,[32] we present a potent biomaterial platform for tunable, disease-specific immunomodulation.

■ ASSOCIATED CONTENT

Supporting Information

The Supporting Information is available free of charge on the ACS Publications website at DOI: 10.1021/acsbiomaterials.9b00332.

Diabetes prevention study using an earlier iteration of the dMP system, representative flow plots, comparisons between soluble factors and factor-loaded MPs in modulating DCs in vitro, in vivo imaging of fluorescent MPs, characterization of the subcutaneous dMP depot at the site of injection, the full eight-group diabetes prevention study with all groups plotted together, insulitis scoring, and rabbit pyrogenicity using the dMP (PDF)

■ AUTHOR INFORMATION

Corresponding Author

*Phone: (352) 273-5878. Fax: (352) 392-9791. E-mail: bgk@ufl.edu. Address: J. Crayton Pruitt Family Department of Biomedical Engineering, P.O. Box 116131, Gainesville, Florida, 32611-6131, U.S.

ORCID

Jamal S. Lewis: 0000-0002-9811-8538

Benjamin G. Keselowsky: 0000-0001-6474-7769

Author Contributions

#J.S.L. and J.M.S. are co-first-authors.

Notes

The authors declare the following competing financial interest(s): J.S.L. and G.P.M. conducted a portion of the reported experiments while employed by OneVax, LLC. C.H.W., T.M.B., M.A.A., and B.G.K. are cofounders of OneVax, LLC, a preclinical biotechnology company with interest in this technology. The authors declare that no other relevant conflicts of interest exist.

■ ACKNOWLEDGMENTS

The authors thank Dr. Maigan Brusko for assisting in flow cytometry training and Noah Barnes for animal upkeep. This work was supported by the National Institutes of Health (Grants R01 DK091658, R01 DK098589, R01 AI133623, R43DK100132, and T32 DK108736).

■ REFERENCES

(1) Atkinson, M. A.; Eisenbarth, G. S.; Michels, A. W. Type 1 diabetes. *Lancet* **2014**, *383* (9911), 69−82.

(2) *National Diabetes Statistics Report, 2014: Estimates of Diabetes and Its Burden in the United States*; Centers for Disease Control and Prevention, U.S. Department of Health and Human Services: Atlanta, GA, 2014.

(3) Bluestone, J. A.; Herold, K.; Eisenbarth, G. Genetics, pathogenesis and clinical interventions in type 1 diabetes. *Nature* **2010**, *464* (7293), 1293−300.

DOI: 10.1021/acsbiomaterials.9b00332
ACS Biomater. Sci. Eng. 2019, 5, 2631−2646

(4) Laing, S. P.; Swerdlow, A. J.; Slater, S. D.; Burden, A. C.; Morris, A.; Waugh, N. R.; Gatling, W.; Bingley, P. J.; Patterson, C. C. Mortality from heart disease in a cohort of 23,000 patients with insulin-treated diabetes. *Diabetologia* **2003**, *46* (6), 760−5.
(5) Groop, P. H.; Thomas, M. C.; Moran, J. L.; Waden, J.; Thorn, L. M.; Makinen, V. P.; Rosengard-Barlund, M.; Saraheimo, M.; Hietala, K.; Heikkila, O.; Forsblom, C. The presence and severity of chronic kidney disease predicts all-cause mortality in type 1 diabetes. *Diabetes* **2009**, *58* (7), 1651−8.
(6) Herold, K. C.; Hagopian, W.; Auger, J. A.; Poumian-Ruiz, E.; Taylor, L.; Donaldson, D.; Gitelman, S. E.; Harlan, D. M.; Xu, D.; Zivin, R. A.; Bluestone, J. A. Anti-CD3 monoclonal antibody in new-onset type 1 diabetes mellitus. *N. Engl. J. Med.* **2002**, *346* (22), 1692−8.
(7) Pescovitz, M. D.; Greenbaum, C. J.; Krause-Steinrauf, H.; Becker, D. J.; Gitelman, S. E.; Goland, R.; Gottlieb, P. A.; Marks, J. B.; McGee, P. F.; Moran, A. M.; Raskin, P.; Rodriguez, H.; Schatz, D. A.; Wherrett, D.; Wilson, D. M.; Lachin, J. M.; Skyler, J. S. Type 1 Diabetes TrialNet Anti, C. D. S. G., Rituximab, B-lymphocyte depletion, and preservation of beta-cell function. *N. Engl. J. Med.* **2009**, *361* (22), 2143−52.
(8) Shapiro, A. M.; Lakey, J. R.; Ryan, E. A.; Korbutt, G. S.; Toth, E.; Warnock, G. L.; Kneteman, N. M.; Rajotte, R. V. Islet transplantation in seven patients with type 1 diabetes mellitus using a glucocorticoid-free immunosuppressive regimen. *N. Engl. J. Med.* **2000**, *343* (4), 230−8.
(9) Voltarelli, J. C.; Couri, C. E.; Stracieri, A. B.; Oliveira, M. C.; Moraes, D. A.; Pieroni, F.; Coutinho, M.; Malmegrim, K. C.; Foss-Freitas, M. C.; Simoes, B. P.; Foss, M. C.; Squiers, E.; Burt, R. K. Autologous nonmyeloablative hematopoietic stem cell transplantation in newly diagnosed type 1 diabetes mellitus. *JAMA* **2007**, *297* (14), 1568−76.
(10) Haller, M. J.; Gitelman, S. E.; Gottlieb, P. A.; Michels, A. W.; Perry, D. J.; Schultz, A. R.; Hulme, M. A.; Shuster, J. J.; Zou, B.; Wasserfall, C. H.; Posgai, A.; Mathews, C. E.; Brusko, T. M.; Atkinson, M. A.; Schatz, D. A. Anti-Thymocyte Globulin Plus G-CSF Combination Therapy Leads to Sustained Immunomodulatory and Metabolic Effects in a Subset of Responders with Established Type 1 Diabetes. *Diabetes* **2016**, *65*, 3765.
(11) Haller, M. J.; Gitelman, S. E.; Gottlieb, P. A.; Michels, A. W.; Rosenthal, S. M.; Shuster, J. J.; Zou, B.; Brusko, T. M.; Hulme, M. A.; Wasserfall, C. H.; Mathews, C. E.; Atkinson, M. A.; Schatz, D. A. Anti-thymocyte globulin/G-CSF treatment preserves beta cell function in patients with established type 1 diabetes. *J. Clin. Invest.* **2015**, *125* (1), 448−55.
(12) Ryan, E. A.; Paty, B. W.; Senior, P. A.; Bigam, D.; Alfadhli, E.; Kneteman, N. M.; Lakey, J. R.; Shapiro, A. M. Five-year follow-up after clinical islet transplantation. *Diabetes* **2005**, *54* (7), 2060−9.
(13) Couri, C. E.; Oliveira, M. C.; Stracieri, A. B.; Moraes, D. A.; Pieroni, F.; Barros, G. M.; Madeira, M. I.; Malmegrim, K. C.; Foss-Freitas, M. C.; Simoes, B. P.; Martinez, E. Z.; Foss, M. C.; Burt, R. K.; Voltarelli, J. C. C-peptide levels and insulin independence following autologous nonmyeloablative hematopoietic stem cell transplantation in newly diagnosed type 1 diabetes mellitus. *JAMA* **2009**, *301* (15), 1573−9.
(14) Sherry, N.; Hagopian, W.; Ludvigsson, J.; Jain, S. M.; Wahlen, J.; Ferry, R. J., Jr.; Bode, B.; Aronoff, S.; Holland, C.; Carlin, D.; King, K. L.; Wilder, R. L.; Pillemer, S.; Bonvini, E.; Johnson, S.; Stein, K. E.; Koenig, S.; Herold, K. C.; Daifotis, A. G. Teplizumab for treatment of type 1 diabetes (Protege study): 1-year results from a randomised, placebo-controlled trial. *Lancet* **2011**, *378* (9790), 487−97.
(15) Caspi, R. R. Immunotherapy of autoimmunity and cancer: the penalty for success. *Nat. Rev. Immunol.* **2008**, *8* (12), 970−6.
(16) Creusot, R. J.; Giannoukakis, N.; Trucco, M.; Clare-Salzler, M. J.; Fathman, C. G. It's time to bring dendritic cell therapy to type 1 diabetes. *Diabetes* **2014**, *63* (1), 20−30.
(17) Lewis, J. S.; Zaveri, T. D.; Crooks, C. P., 2nd; Keselowsky, B. G. Microparticle surface modifications targeting dendritic cells for non-activating applications. *Biomaterials* **2012**, *33* (29), 7221−32.
(18) Banchereau, J.; Steinman, R. M. Dendritic cells and the control of immunity. *Nature* **1998**, *392* (6673), 245−252.
(19) Jansen, A.; van Hagen, M.; Drexhage, H. A. Defective maturation and function of antigen-presenting cells in type 1 diabetes. *Lancet* **1995**, *345* (8948), 491−2.
(20) Price, J. D.; Tarbell, K. V. The Role of Dendritic Cell Subsets and Innate Immunity in the Pathogenesis of Type 1 Diabetes and Other Autoimmune Diseases. *Front. Immunol.* **2015**, *6*, 288.
(21) Steinman, R. M.; Hawiger, D.; Nussenzweig, M. C. Tolerogenic dendritic cells. *Annu. Rev. Immunol.* **2003**, *21*, 685−711.
(22) Phillips, B. E.; Garciafigueroa, Y.; Trucco, M.; Giannoukakis, N. Clinical Tolerogenic Dendritic Cells: Exploring Therapeutic Impact on Human Autoimmune Disease. *Front. Immunol.* **2017**, *8*, 1279.
(23) Tacken, P. J.; de Vries, I. J.; Torensma, R.; Figdor, C. G. Dendritic-cell immunotherapy: from ex vivo loading to in vivo targeting. *Nat. Rev. Immunol.* **2007**, *7* (10), 790−802.
(24) MartIn-Fontecha, A.; Sebastiani, S.; Hopken, U. E.; Uguccioni, M.; Lipp, M.; Lanzavecchia, A.; Sallusto, F. Regulation of dendritic cell migration to the draining lymph node: impact on T lymphocyte traffic and priming. *J. Exp. Med.* **2003**, *198* (4), 615−21.
(25) Stewart, J. M.; Keselowsky, B. G. Combinatorial drug delivery approaches for immunomodulation. *Adv. Drug Delivery Rev.* **2017**, *114*, 161−174.
(26) Bracho-Sanchez, E.; Xia, C. Q.; Clare-Salzler, M. J.; Keselowsky, B. G. Micro and Nano Material Carriers for Immunomodulation. *Am. J. Transplant.* **2016**, *16*, 3362.
(27) Keselowsky, B. G.; Xia, C. Q.; Clare-Salzler, M. Multifunctional dendritic cell-targeting polymeric microparticles: engineering new vaccines for type 1 diabetes. *Hum. Vaccines* **2011**, *7* (1), 37−44.
(28) Phillips, B.; Nylander, K.; Harnaha, J.; Machen, J.; Lakomy, R.; Styche, A.; Gillis, K.; Brown, L.; Lafreniere, D.; Gallo, M.; Knox, J.; Hogeland, K.; Trucco, M.; Giannoukakis, N. A microsphere-based vaccine prevents and reverses new-onset autoimmune diabetes. *Diabetes* **2008**, *57* (6), 1544−55.
(29) Maldonado, R. A.; LaMothe, R. A.; Ferrari, J. D.; Zhang, A. H.; Rossi, R. J.; Kolte, P. N.; Griset, A. P.; O'Neil, C.; Altreuter, D. H.; Browning, E.; Johnston, L.; Farokhzad, O. C.; Langer, R.; Scott, D. W.; von Andrian, U. H.; Kishimoto, T. K. Polymeric synthetic nanoparticles for the induction of antigen-specific immunological tolerance. *Proc. Natl. Acad. Sci. U. S. A.* **2015**, *112* (2), E156−65.
(30) Allen, R. P.; Bolandparvaz, A.; Ma, J. A.; Manickam, V. A.; Lewis, J. S. Latent, Immunosuppressive Nature of Poly(lactic-co-glycolic acid) Microparticles. *ACS Biomater. Sci. Eng.* **2018**, *4* (3), 900−918.
(31) Lewis, J. S.; Dolgova, N. V.; Zhang, Y.; Xia, C. Q.; Wasserfall, C. H.; Atkinson, M. A.; Clare-Salzler, M. J.; Keselowsky, B. G. A combination dual-sized microparticle system modulates dendritic cells and prevents type 1 diabetes in prediabetic NOD mice. *Clin. Immunol.* **2015**, *160*, 90.
(32) Cho, J. J.; Stewart, J. M.; Drashansky, T. T.; Brusko, M. A.; Zuniga, A. N.; Lorentsen, K. J.; Keselowsky, B. G.; Avram, D. An antigen-specific semi-therapeutic treatment with local delivery of tolerogenic factors through a dual-sized microparticle system blocks experimental autoimmune encephalomyelitis. *Biomaterials* **2017**, *143*, 79−92.
(33) Ali, O. A.; Huebsch, N.; Cao, L.; Dranoff, G.; Mooney, D. J. Infection-mimicking materials to program dendritic cells in situ. *Nat. Mater.* **2009**, *8* (2), 151−8.
(34) Esebanmen, G. E.; Langridge, W. H. R. The role of TGF-beta signaling in dendritic cell tolerance. *Immunol. Res.* **2017**, *65* (5), 987−994.
(35) Roep, B. O.; Peakman, M. Antigen targets of type 1 diabetes autoimmunity. *Cold Spring Harbor Perspect. Med.* **2012**, *2* (4), a007781.
(36) Takiishi, T.; Van Belle, T.; Gysemans, C.; Mathieu, C. Effects of vitamin D on antigen-specific and non-antigen-specific immune modulation: relevance for type 1 diabetes. *Pediatr. Diabetes* **2013**, *14* (2), 81−9.

DOI: 10.1021/acsbiomaterials.9b00332
ACS Biomater. Sci. Eng. 2019, 5, 2631−2646

(37) Oyane, A.; Kim, H. M.; Furuya, T.; Kokubo, T.; Miyazaki, T.; Nakamura, T. Preparation and assessment of revised simulated body fluids. *J. Biomed. Mater. Res.* **2003**, *65A* (2), 188−95.
(38) Acharya, A. P.; Carstens, M. R.; Lewis, J. S.; Dolgova, N.; Xia, C. Q.; Clare-Salzler, M. J.; Keselowsky, B. G. A cell-based microarray to investigate combinatorial effects of microparticle-encapsulated adjuvants on dendritic cell activation. *J. Mater. Chem. B* **2016**, *4* (9), 1672−1685.
(39) Lewis, J. S.; Roche, C.; Zhang, Y.; Brusko, T. M.; Wasserfall, C. H.; Atkinson, M.; Clare-Salzler, M. J.; Keselowsky, B. G. Combinatorial delivery of immunosuppressive factors to dendritic cells using dual-sized microspheres. *J. Mater. Chem. B* **2014**, *2* (17), 2562−2574.
(40) Chen, W.; Jin, W.; Hardegen, N.; Lei, K. J.; Li, L.; Marinos, N.; McGrady, G.; Wahl, S. M. Conversion of peripheral CD4+CD25- naive T cells to CD4+CD25+ regulatory T cells by TGF-beta induction of transcription factor Foxp3. *J. Exp. Med.* **2003**, *198* (12), 1875−86.
(41) Inoue, Y.; Izawa, K.; Kiryu, S.; Tojo, A.; Ohtomo, K. Diet and abdominal autofluorescence detected by in vivo fluorescence imaging of living mice. *Mol. Imaging* **2008**, *7* (1), 21−7.
(42) Miyazaki, A.; Hanafusa, T.; Yamada, K.; Miyagawa, J.; Fujino-Kurihara, H.; Nakajima, H.; Nonaka, K.; Tarui, S. Predominance of T lymphocytes in pancreatic islets and spleen of pre-diabetic non-obese diabetic (NOD) mice: a longitudinal study. *Clin. Exp. Immunol.* **1985**, *60* (3), 622−30.
(43) Pearson, J. A.; Wong, F. S.; Wen, L. The importance of the Non Obese Diabetic (NOD) mouse model in autoimmune diabetes. *J. Autoimmun.* **2016**, *66*, 76−88.
(44) Prasad, S.; Kohm, A. P.; McMahon, J. S.; Luo, X.; Miller, S. D. Pathogenesis of NOD diabetes is initiated by reactivity to the insulin B chain 9−23 epitope and involves functional epitope spreading. *J. Autoimmun.* **2012**, *39* (4), 347−53.
(45) Mellor, A. L.; Munn, D. H. IDO expression by dendritic cells: tolerance and tryptophan catabolism. *Nat. Rev. Immunol.* **2004**, *4* (10), 762−74.
(46) Yoshida, R.; Hayaishi, O. Induction of pulmonary indoleamine 2,3-dioxygenase by intraperitoneal injection of bacterial lipopolysaccharide. *Proc. Natl. Acad. Sci. U. S. A.* **1978**, *75* (8), 3998−4000.
(47) Jones, A.; Bourque, J.; Kuehm, L.; Opejin, A.; Teague, R. M.; Gross, C.; Hawiger, D. Immunomodulatory Functions of BTLA and HVEM Govern Induction of Extrathymic Regulatory T Cells and Tolerance by Dendritic Cells. *Immunity* **2016**, *45* (5), 1066−1077.
(48) Pugliese, A. Insulitis in the pathogenesis of type 1 diabetes. *Pediatr. Diabetes* **2016**, *17* (Suppl.22), 31−6.
(49) Bonifacio, E.; Lampasona, V.; Bernasconi, L.; Ziegler, A. G. Maturation of the humoral autoimmune response to epitopes of GAD in preclinical childhood type 1 diabetes. *Diabetes* **2000**, *49* (2), 202−8.
(50) Pozzilli, P.; Maddaloni, E.; Buzzetti, R. Combination immunotherapies for type 1 diabetes mellitus. *Nat. Rev. Endocrinol.* **2015**, *11* (5), 289−97.
(51) Stewart, J. M.; Keselowsky, B. G. Combinatorial drug delivery approaches for immunomodulation. *Adv. Drug Delivery Rev.* **2017**, *114*, 161.
(52) Larkin, J.; Chiarion-Sileni, V.; Gonzalez, R.; Grob, J. J.; Cowey, C. L.; Lao, C. D.; Schadendorf, D.; Dummer, R.; Smylie, M.; Rutkowski, P.; Ferrucci, P. F.; Hill, A.; Wagstaff, J.; Carlino, M. S.; Haanen, J. B.; Maio, M.; Marquez-Rodas, I.; McArthur, G. A.; Ascierto, P. A.; Long, G. V.; Callahan, M. K.; Postow, M. A.; Grossmann, K.; Sznol, M.; Dreno, B.; Bastholt, L.; Yang, A.; Rollin, L. M.; Horak, C.; Hodi, F. S.; Wolchok, J. D. Combined Nivolumab and Ipilimumab or Monotherapy in Untreated Melanoma. *N. Engl. J. Med.* **2015**, *373* (1), 23−34.
(53) Wolchok, J. D.; Kluger, H.; Callahan, M. K.; Postow, M. A.; Rizvi, N. A.; Lesokhin, A. M.; Segal, N. H.; Ariyan, C. E.; Gordon, R. A.; Reed, K.; Burke, M. M.; Caldwell, A.; Kronenberg, S. A.; Agunwamba, B. U.; Zhang, X.; Lowy, I.; Inzunza, H. D.; Feely, W.; Horak, C. E.; Hong, Q.; Korman, A. J.; Wigginton, J. M.; Gupta, A.; Sznol, M. Nivolumab plus ipilimumab in advanced melanoma. *N. Engl. J. Med.* **2013**, *369* (2), 122−33.
(54) Tostanoski, L. H.; Chiu, Y. C.; Gammon, J. M.; Simon, T.; Andorko, J. I.; Bromberg, J. S.; Jewell, C. M. Reprogramming the Local Lymph Node Microenvironment Promotes Tolerance that Is Systemic and Antigen Specific. *Cell Rep.* **2016**, *16* (11), 2940−52.
(55) Andorko, J. I.; Tostanoski, L. H.; Solano, E.; Mukhamedova, M.; Jewell, C. M. Intra-lymph node injection of biodegradable polymer particles. *J. Visualized Exp.* **2014**, No. 83, No. e50984.
(56) Jewell, C. M.; Bustamante Lopez, S. C.; Irvine, D. J. In situ engineering of the lymph node microenvironment via intranodal injection of adjuvant-releasing polymer particles. *Proc. Natl. Acad. Sci. U. S. A.* **2011**, *108* (38), 15745−50.
(57) Ben Nasr, M.; Tezza, S.; D'Addio, F.; Mameli, C.; Usuelli, V.; Maestroni, A.; Corradi, D.; Belletti, S.; Albarello, L.; Becchi, G.; Fadini, G. P.; Schuetz, C.; Markmann, J.; Wasserfall, C.; Zon, L.; Zuccotti, G. V.; Fiorina, P. PD-L1 genetic overexpression or pharmacological restoration in hematopoietic stem and progenitor cells reverses autoimmune diabetes. *Sci. Transl. Med.* **2017**, *9* (416), eaam7543.
(58) Stamatouli, A. M.; Quandt, Z.; Perdigoto, A. L.; Clark, P. L.; Kluger, H.; Weiss, S. A.; Gettinger, S.; Sznol, M.; Young, A.; Rushakoff, R.; Lee, J.; Bluestone, J. A.; Anderson, M.; Herold, K. C. Collateral Damage: Insulin-Dependent Diabetes Induced With Checkpoint Inhibitors. *Diabetes* **2018**, *67* (8), 1471−1480.
(59) Insel, R. A.; Dunne, J. L.; Atkinson, M. A.; Chiang, J. L.; Dabelea, D.; Gottlieb, P. A.; Greenbaum, C. J.; Herold, K. C.; Krischer, J. P.; Lernmark, A.; Ratner, R. E.; Rewers, M. J.; Schatz, D. A.; Skyler, J. S.; Sosenko, J. M.; Ziegler, A. G. Staging presymptomatic type 1 diabetes: a scientific statement of JDRF, the Endocrine Society, and the American Diabetes Association. *Diabetes Care* **2015**, *38* (10), 1964−74.
(60) Watkins, R. A.; Evans-Molina, C.; Blum, J. S.; DiMeglio, L. A. Established and emerging biomarkers for the prediction of type 1 diabetes: a systematic review. *Transl. Res.* **2014**, *164* (2), 110−21.
(61) Koup, R. A.; Douek, D. C. Vaccine design for CD8 T lymphocyte responses. *Cold Spring Harbor Perspect. Med.* **2011**, *1* (1), a007252.
(62) Shen, H.; Ackerman, A. L.; Cody, V.; Giodini, A.; Hinson, E. R.; Cresswell, P.; Edelson, R. L.; Saltzman, W. M.; Hanlon, D. J. Enhanced and prolonged cross-presentation following endosomal escape of exogenous antigens encapsulated in biodegradable nanoparticles. *Immunology* **2006**, *117* (1), 78−88.
(63) Gutierrez-Martinez, E.; Planes, R.; Anselmi, G.; Reynolds, M.; Menezes, S.; Adiko, A. C.; Saveanu, L.; Guermonprez, P. Cross-Presentation of Cell-Associated Antigens by MHC Class I in Dendritic Cell Subsets. *Front. Immunol.* **2015**, *6*, 363.
(64) Grinberg-Bleyer, Y.; Baeyens, A.; You, S.; Elhage, R.; Fourcade, G.; Gregoire, S.; Cagnard, N.; Carpentier, W.; Tang, Q.; Bluestone, J.; Chatenoud, L.; Klatzmann, D.; Salomon, B. L.; Piaggio, E. IL-2 reverses established type 1 diabetes in NOD mice by a local effect on pancreatic regulatory T cells. *J. Exp. Med.* **2010**, *207* (9), 1871−8.
(65) Wang, P.; Fiaschi-Taesch, N. M.; Vasavada, R. C.; Scott, D. K.; Garcia-Ocana, A.; Stewart, A. F. Diabetes mellitus−advances and challenges in human beta-cell proliferation. *Nat. Rev. Endocrinol.* **2015**, *11* (4), 201−12.
(66) Shen, W.; Taylor, B.; Jin, Q.; Nguyen-Tran, V.; Meeusen, S.; Zhang, Y. Q.; Kamireddy, A.; Swafford, A.; Powers, A. F.; Walker, J.; Lamb, J.; Bursalaya, B.; DiDonato, M.; Harb, G.; Qiu, M.; Filippi, C. M.; Deaton, L.; Turk, C. N.; Suarez-Pinzon, W. L.; Liu, Y.; Hao, X.; Mo, T.; Yan, S.; Li, J.; Herman, A. E.; Hering, B. J.; Wu, T.; Martin Seidel, H.; McNamara, P.; Glynne, R.; Laffitte, B. Inhibition of DYRK1A and GSK3B induces human beta-cell proliferation. *Nat. Commun.* **2015**, *6*, 8372.
(67) Mathieu, C.; Waer, M.; Casteels, K.; Laureys, J.; Bouillon, R. Prevention of type I diabetes in NOD mice by nonhypercalcemic doses of a new structural analog of 1,25-dihydroxyvitamin D3, KH1060. *Endocrinology* **1995**, *136* (3), 866−72.

DOI: 10.1021/acsbiomaterials.9b00332
ACS Biomater. Sci. Eng. 2019, 5, 2631−2646

(68) Mathieu, C.; Laureys, J.; Sobis, H.; Vandeputte, M.; Waer, M.; Bouillon, R. 1,25-Dihydroxyvitamin D3 prevents insulitis in NOD mice. *Diabetes* **1992**, *41* (11), 1491−5.
(69) Gregori, S.; Giarratana, N.; Smiroldo, S.; Uskokovic, M.; Adorini, L. A 1alpha,25-dihydroxyvitamin D(3) analog enhances regulatory T-cells and arrests autoimmune diabetes in NOD mice. *Diabetes* **2002**, *51* (5), 1367−74.
(70) Mansilla, M. J.; Contreras-Cardone, R.; Navarro-Barriuso, J.; Cools, N.; Berneman, Z.; Ramo-Tello, C.; Martinez-Caceres, E. M. Cryopreserved vitamin D3-tolerogenic dendritic cells pulsed with autoantigens as a potential therapy for multiple sclerosis patients. *J. Neuroinflammation* **2016**, *13* (1), 113.
(71) Mansilla, M. J.; Selles-Moreno, C.; Fabregas-Puig, S.; Amoedo, J.; Navarro-Barriuso, J.; Teniente-Serra, A.; Grau-Lopez, L.; Ramo-Tello, C.; Martinez-Caceres, E. M. Beneficial effect of tolerogenic dendritic cells pulsed with MOG autoantigen in experimental autoimmune encephalomyelitis. *CNS Neurosci. Ther.* **2015**, *21* (3), 222−30.
(72) Stoop, J. N.; Harry, R. A.; von Delwig, A.; Isaacs, J. D.; Robinson, J. H.; Hilkens, C. M. Therapeutic effect of tolerogenic dendritic cells in established collagen-induced arthritis is associated with a reduction in Th17 responses. *Arthritis Rheum.* **2010**, *62* (12), 3656−65.
(73) Verbeke, C. S.; Gordo, S.; Schubert, D. A.; Lewin, S. A.; Desai, R. M.; Dobbins, J.; Wucherpfennig, K. W.; Mooney, D. J. Multicomponent Injectable Hydrogels for Antigen-Specific Tolerogenic Immune Modulation. *Adv. Healthcare Mater.* **2017**, *6*, 1600773.
(74) Prasad, S.; Neef, T.; Xu, D.; Podojil, J. R.; Getts, D. R.; Shea, L. D.; Miller, S. D. Tolerogenic Ag-PLG nanoparticles induce tregs to suppress activated diabetogenic CD4 and CD8 T cells. *J. Autoimmun.* **2018**, *89*, 112.
(75) Getts, D. R.; Turley, D. M.; Smith, C. E.; Harp, C. T.; McCarthy, D.; Feeney, E. M.; Getts, M. T.; Martin, A. J.; Luo, X.; Terry, R. L.; King, N. J.; Miller, S. D. Tolerance induced by apoptotic antigen-coupled leukocytes is induced by PD-L1+ and IL-10-producing splenic macrophages and maintained by T regulatory cells. *J. Immunol.* **2011**, *187* (5), 2405−17.

DOI: 10.1021/acsbiomaterials.9b00332
ACS Biomater. Sci. Eng. 2019, 5, 2631−2646